Journal of Computational and Applied Mathematics 301 (2016) 241–258

Contents lists available at ScienceDirect

Journal of Computational and Applied Mathematics

journal homepage: www.elsevier.com/locate/cam

Hierarchical high order finite element bases for **H**(div) spaces based on curved meshes for two-dimensional regions or manifolds

Douglas A. Castro [a,*], Philippe R.B. Devloo [b], Agnaldo M. Farias [c], Sônia M. Gomes [c], Omar Durán [d]

[a] *Universidade Federal do Tocantins - Campus Gurupi, TO, Brazil*
[b] *FEC-Universidade Estadul de Campinas, Campinas-SP, Brazil*
[c] *IMECC-Universidade Estadual de Campinas, Campinas-SP, Brazil*
[d] *FEM-Universidade Estadual de Campinas, Campinas-SP, Brazil*

HIGHLIGHTS

- Innovative two dimensional Hdiv approximation spaces for curved quadrilateral and triangular elements.
- Hdiv bases properly constructed on the master element and mapped to the geometrical elements by the Piola transformation, followed by a normalization procedure.
- Stable convergence with optimal convergence rates, coinciding for primal and dual variables.
- Study of number of condensed equations as a function of the polynomial order of the shape functions.

ARTICLE INFO

Article history:
Received 12 July 2015
Received in revised form 13 December 2015

Keywords:
Mixed finite elements
Approximation spaces
Hdiv spaces
Manifold domain

ABSTRACT

The mixed finite element formulation for elliptic problems is characterized by simultaneous calculations of the potential (primal variable) and of the flux field (dual variable). This work focuses on new **H**(div)-conforming finite element spaces, which are suitable for flux approximations, based on curved meshes of a planar region or a manifold domain embedded in $\mathbb{R}^3$. The adopted methodology for the construction of **H**(div) bases consists in using hierarchical H^1-conforming scalar bases multiplied by vector fields that are properly constructed on the master element and mapped to the geometrical elements by the Piola transformation, followed by a normalization procedure. They are classified as being of edge or internal type. The normal component of an edge function coincides on the corresponding edge with the associated scalar shape function, and vanishes over the other edges, and the normal components of an internal shape function vanishes on all element edges. These properties are fundamental for the global assembly of **H**(div)-conforming functions locally defined by these vectorial shape functions. For applications to the mixed formulation, the configuration of the approximation spaces is such that the divergence of the dual space and the primal approximation space coincides. Results of verification numerical tests are presented for curved triangular and quadrilateral partitions on circular, cylindrical and spherical regions, demonstrating stable convergence with optimal convergence rates, coinciding for primal and dual variables.

* Corresponding author. Tel.: +55 63 33113512.
E-mail addresses: dacastro@mail.uft.edu.br (D.A. Castro), phil@fec.unicamp.br (P.R.B. Devloo), agnaldofarias.mg@gmail.com (A.M. Farias), soniag@ime.unicamp.br (S.M. Gomes), omaryesiduran@gmail.com (O. Durán).

http://dx.doi.org/10.1016/j.cam.2016.01.053
0377-0427/

1. Introduction

The mixed method [1] is a classical formulation for flow simulations, which is based on simultaneous calculations of the potential (primal variable) and of the flux field (dual variable). The appropriate finite element approximation spaces for the flux field are of $\mathbf{H}(\mathrm{div})$ type, formed by vectorial functions, not necessarily continuous, but with continuous normal components at the interfaces of the elements. Discontinuous finite element spaces are used for potential approximations. These properties are crucial to ensure local mass conservation, a fundamental requirement in this type of application.

Many conservation laws can be defined on manifolds, such as thermal flow simulation over shells (e.g. satellites) and simulations of the atmosphere where the computational domain is a sphere. Other areas can be simulations of electrical currents over conductive surfaces. In most of these problems the local conservation of the quantity of interest is crucial.

The main objective of this work is to build hierarchical high order shape functions for finite element subspaces of $\mathbf{H}(\mathrm{div})$ type based on partitions $\Gamma = K$ of the computational domain Ω, where K is a curved triangular or quadrilateral element. The domain Ω may be a region contained in the Euclidean space $\mathbb{R}^2$ or a manifold immersed in $\mathbb{R}^3$.

Since the pioneering work by Raviart and Thomas [2] in 1977, different constructions of $\mathbf{H}(\mathrm{div})$ (or $\mathbf{H}(\mathrm{curl})$) approximation space have been proposed in the literature. In some contexts the vector basis functions are constructed on the master element and then they are transformed to the elements of the partition by Piola transformations, as described in [1,3,4]. Recent constructions of hierarchical high order spaces, as described in [5–9], are based on the properties of the De Rham complex, and require the computations of gradients of scalar functions in H^1- conforming spaces. Piola transformation for affine mappings of regions $\Omega \subset \mathbb{R}^2$ or $\Omega \subset \mathbb{R}^3$ has been used in [3] to map traditional RT_{k-1} and BDM_k bases, for $k = 1, 2$, defined in triangular or tetrahedral master elements. In [10], the method is used for two-dimensional elements over a manifold of $\mathbb{R}^3$, with affine mappings and bases RT_{k-1}, BDM_k and $BDFM_k$.

The methodology proposed in the present paper for the construction of $\mathbf{H}(\mathrm{div})$ bases consists in using hierarchical H^1-conforming scalar bases multiplied by vector fields that are properly constructed on the master element and mapped to the geometrical elements by the Piola transformation, followed by a normalization procedure. For triangular and quadrilateral elements with straight sides, similar methodology has been successfully applied in [11], but there the vector fields are constructed directly on the geometric elements, without using Piola transformations.

This methodology for the construction of $\mathbf{H}(\mathrm{div})$-conforming functions is designed having in mind the resources provided by NeoPZ [12], where the required hierarchical high order continuous scalar basis functions are already implemented for conformal or non-conformal *hp*-meshes [13,14]. NeoPZ is a general finite element approximation library organized by modules for broad classes of technologies, incorporating a variety of element geometries, variational formulations, and approximation spaces (e.g. continuous, discontinuous, $\mathbf{H}(\mathrm{div})$-conforming, and others). It allows the user to apply *hp*-strategies by choosing locally the mesh refinement and the order of approximation. NeoPZ is integrated with pthreads and thread building blocks for efficient execution on multi core computers. Multiphysics simulations can also be implemented by combining different approximation spaces into a coupled system of equations [15], a procedure that facilitates the implementations of mixed formulations based on different approximation spaces for dual and primal variables.

The paper is organized as follows. Section 2 summarizes the main steps in the construction of the vectorial shape functions of $\mathbf{H}(\mathrm{div})$ type. The next three sections are dedicated to give the details of these steps. The main properties of the required hierarchical scalar bases and of the family of constant vector fields in the master elements are presented in Section 3. In Section 4, the geometric mappings and the associated transformations of scalar functions from the master element to the geometric elements are described, as well as the procedure for the construction of H^1-conforming approximation spaces. The main part of this paper is Section 5, where a detailed construction of the vectorial $\mathbf{H}(\mathrm{div})$ shape functions at element level over partitions by curved elements is described, and their global assembly over the domain, guaranteeing the continuity of normal components across element interfaces. The results of the applications of these bases for the representation of flux fields on discrete formulations of the mixed method are discussed in Section 6 for three test problems defined on circular, cylindrical and spherical computational domains. Section 7 gives the final conclusions of the article.

2. Script

For each two-dimensional curved geometric element K, flat when $K \subset \mathbb{R}^2$ or on a manifold immersed in $\mathbb{R}^3$, the construction of bases $\mathbf{B}_k^K$ for subspaces of $\mathbf{H}(\mathrm{div}, K)$ follows a common script, considering the following aspects:

1. A master element $\hat{K} \subset \mathbb{R}^2$ (triangular or quadrilateral), and a geometric mapping $\mathbf{x} : \hat{K} \to K$, associating each point $\boldsymbol{\xi}$ in the master element to a point $\mathbf{p} = \mathbf{x}(\boldsymbol{\xi})$ in the geometric element.
2. A polynomial space $\mathcal{P}_k$, where the parameter k refers to the degree of the polynomial, and a scalar hierarchical base $\hat{\mathcal{B}}_k = \{\hat{\varphi}\}$ of $\mathcal{P}_k$. Each basic functions $\hat{\varphi}$ is associated to one of the basic elements of $\hat{K}$: vertex, edge or to $\hat{K}$ itself.
3. Constant vector fields $\hat{\mathbf{b}}$ defined over the master element. These fields are classified as being of edge or internal type. A field associated to a given edge is incident to it, and is connected to one of its basic elements: vertex or the edge itself. The internal fields may be connected to the interior of the master element or to fields tangent to an edge.
4. A transformation $\mathbb{F} : \hat{\varphi} \to \varphi$, an isomorphism mapping scalar functions of $H^1(\hat{K})$ to scalar functions of $H^1(K)$, which is induced by the geometric mapping.

5. Construction of hierarchical bases $\mathcal{B}_k^K = \{\varphi\}$ for subspaces of $H^1(K)$. Each scalar shape function φ has the form $\varphi = \mathbb{F}[\hat{\varphi}(\tilde{\boldsymbol{\xi}})]$, where $\hat{\varphi} \in \hat{\mathcal{B}}_k$. For each scalar shape function, there is an appropriate parametrization $\tilde{\boldsymbol{\xi}}$ of $\hat{K}$, a key tool to ensure continuity at element interfaces, when the scalar shape functions are combined to form a subspace in $H^1(\Omega)$.
6. The geometric mapping also induces a contravariant Piola transformation $\mathbb{F}^{div} : \hat{\boldsymbol{\Phi}} \to \boldsymbol{\Phi}$, an isomorphism mapping vector fields $\hat{\boldsymbol{\Phi}} \in \mathbf{H}(\mathrm{div}, \hat{K})$ to vector fields $\boldsymbol{\Phi} \in \mathbf{H}(\mathrm{div}, K)$.
7. Construction of vector fields $\mathbf{b}$ defined over K by the Piola transformation $\mathbb{F}^{div}\hat{\mathbf{b}}$ of the vector fields $\hat{\mathbf{b}}$ mentioned in Item 3. Accordingly, the fields $\mathbf{b}$ are also classified as being of edge or interior type, in accordance with the classification of the corresponding vector fields $\hat{\mathbf{b}}$.
8. Construction of a basis $\mathbf{B}_k^K = \{\boldsymbol{\Phi}\}$ for a subspace in $\mathbf{H}(\mathrm{div}, K)$. Each vectorial shape function $\boldsymbol{\Phi}$ has the form

$$\boldsymbol{\Phi} = \varphi\mathbf{v},$$

where φ is a scalar basic function in $\mathcal{B}_k^K$ and $\mathbf{v}$ is obtained by a normalization procedure of a field $\mathbf{b}$. Normalization is done in order to ensure the unitary normal component of an edge field $\mathbf{v}$ over its associated edge. Internal fields do not require such normalization. The properties of the normal components of $\mathbf{v}$ over the edges of K, combined with the continuity of scalar shape functions φ are fundamental for the global assembly of $\mathbf{H}(\mathrm{div})$-conforming functions locally generated by the bases $\mathbf{B}_k^K$, in each element of the partition.

Detailed descriptions of these steps are presented in the next three sections.

3. Scalar bases and constant vector fields at the master element

This section contains the descriptions of Items 1, 2, and 3 listed in the previous Script section.

3.1. Master element and polynomial spaces

Let $\hat{K} \subset \mathbb{R}^2$ be a quadrilateral or triangular master element. Its basic lower dimension elements are the vertices $\hat{a}_m$ and edges $\hat{l}_m$, as described in Fig. 3.1. Denote by $\hat{\mathcal{V}}$ and $\hat{\mathcal{A}}$ the sets of vertices and edges of $\hat{K}$, respectively. Let $\hat{\mathbf{n}}$ denote the unitary external normal to $\hat{K}$. Two edges are said to be adjacent if they share a vertex.

Quadrilateral master element The quadrilateral master element is

$$\hat{K} = \{(\xi_0, \xi_1) : -1 \le \xi_0, \xi_1 \le 1\},$$

with vertices $\hat{a}_0 = (-1, -1)$, $\hat{a}_1 = (1, -1)$, $\hat{a}_2 = (1, 1)$ and $\hat{a}_3 = (-1, 1)$. The edges $\hat{l}_m$, $m = 0, 1, 2$ and 3, are given by the segments connecting the vertices $\hat{a}_m$ a $\hat{a}_{m+1 \pmod 4}$. The spaces $\mathcal{P}_k = \mathcal{Q}_k(\hat{K})$ are the polynomials with degree at most k for each variable, with dimension $(k+1)^2$. That is, a polynomial $p \in \mathcal{Q}_k(\hat{K})$ has the tensorial form

$$p(\xi_0, \xi_1) = \sum_{i,j \le k} a_{ij}\xi_0^i\xi_1^j.$$

Triangular master element The triangular master element is

$$\hat{K} = \{(\xi_0, \xi_1),\ 0 \le \xi_0 \le 1,\ 0 \le \xi_1 \le 1 - \xi_0\},$$

with vertices $\hat{a}_0 = (0, 0)$, $\hat{a}_1 = (1, 0)$, $\hat{a}_2 = (0, 1)$. Its edges $\hat{l}_m$, $m = 0$, 1 and 2, are given by the segments connecting the vertices $\hat{a}_m$ a $\hat{a}_{m+1 \pmod 3}$. The spaces $\mathcal{P}_k$ are formed by polynomials of total degree k, with dimension equal to $\frac{1}{2}(k+1)(k+2)$. A polynomial $p \in \mathcal{P}_k$ has the form

$$p(\xi_0, \xi_1) = \sum_{i,j,\ i+j \le k} a_{ij}\xi_0^i\xi_1^j.$$

3.2. Scalar hierarchical bases for the polynomial spaces on the master element

As shown in [13], hierarchical bases $\hat{\mathcal{B}}_k$ for the polynomial spaces $\mathcal{P}_k$ are formed by shape functions classified as:

- **Vertex functions** $\hat{\varphi}^{\hat{a}_m}(\boldsymbol{\xi})$, such that $\hat{\varphi}^{\hat{a}_m}(\hat{a}_s) = \delta_{ms}$ (and vanishing at all edges that do not share $\hat{a}_m$).
- **Edge functions** $\hat{\varphi}^{\hat{l}_m,n}(\boldsymbol{\xi})$, vanishing at all edges $\hat{l}_s$, with $s \neq m$, and in all vertices.
- **Internal functions** $\hat{\varphi}^{\hat{K},n_1,n_2}(\boldsymbol{\xi})$, vanishing at all edges and vertices.

The vertex functions are traditional first order Lagrangian bases. The other ones (of edge and internal types) are defined by the multiplication of one-dimensional Chebyshev polynomials with quadratic functions (*blending functions*), formed by the combination of vertex functions. Chebyshev polynomials are defined recursively by

$$f_0(t) = 1,$$
$$f_1(t) = t,$$
$$f_n(t) = 2tf_{n-1}(t) - f_{n-2}(t), \quad n \ge 2.$$

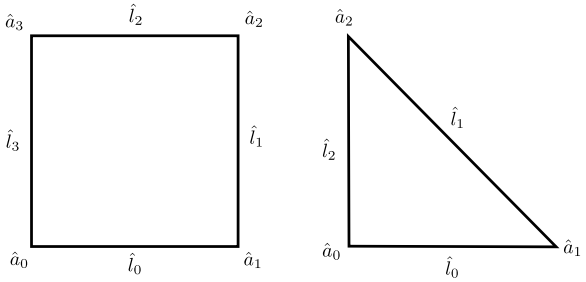

Fig. 3.1. Quadrilateral and triangular master elements, and their vertices and edges.

Quadrilateral Case

A hierarchical polynomial basis for $\mathcal{P}_k = \mathcal{Q}_k(\hat{K})$, of dimension $(k+1)^2$, is formed by:

- 4 vertex functions $\hat{\varphi}^{\hat{a}_m}$:

$$\hat{\varphi}^{\hat{a}_0}(\xi_0,\xi_1) = \frac{(1-\xi_0)}{2}\frac{(1-\xi_1)}{2}, \qquad \hat{\varphi}^{\hat{a}_1}(\xi_0,\xi_1) = \frac{(1+\xi_0)}{2}\frac{(1-\xi_1)}{2},$$
$$\hat{\varphi}^{\hat{a}_2}(\xi_0,\xi_1) = \frac{(1+\xi_0)}{2}\frac{(1+\xi_1)}{2}, \qquad \hat{\varphi}^{\hat{a}_3}(\xi_0,\xi_1) = \frac{(1-\xi_0)}{2}\frac{(1+\xi_1)}{2},$$

  such that $\varphi^{\hat{a}_m}(\hat{a}_s) = \delta_{ms}$ and vanishing on the edge that does not share the vertex $\hat{a}_m$.
- $4(k-1)$ edge functions, $\hat{\varphi}^{\hat{l}_m,n}$, for $k \geq 2$, $n = 0, 1, \ldots, k-2$:

$$\hat{\varphi}^{\hat{l}_0,n}(\xi_0,\xi_1) = \hat{\varphi}^{\hat{a}_0}(\xi_0,\xi_1)[\hat{\varphi}^{\hat{a}_1}(\xi_0,\xi_1) + \hat{\varphi}^{\hat{a}_2}(\xi_0,\xi_1)]f_n(\xi_0),$$
$$\hat{\varphi}^{\hat{l}_1,n}(\xi_0,\xi_1) = \hat{\varphi}^{\hat{a}_1}(\xi_0,\xi_1)[\hat{\varphi}^{\hat{a}_2}(\xi_0,\xi_1) + \hat{\varphi}^{\hat{a}_3}(\xi_0,\xi_1)]f_n(\xi_1),$$
$$\hat{\varphi}^{\hat{l}_2,n}(\xi_0,\xi_1) = \hat{\varphi}^{\hat{a}_2}(\xi_0,\xi_1)[\hat{\varphi}^{\hat{a}_3}(\xi_0,\xi_1) + \hat{\varphi}^{\hat{a}_0}(\xi_0,\xi_1)]f_n(-\xi_0),$$
$$\hat{\varphi}^{\hat{l}_3,n}(\xi_0,\xi_1) = \hat{\varphi}^{\hat{a}_3}(\xi_0,\xi_1)[\hat{\varphi}^{\hat{a}_0}(\xi_0,\xi_1) + \hat{\varphi}^{\hat{a}_1}(\xi_0,\xi_1)]f_n(-\xi_1).$$

  The edge functions $\hat{\varphi}^{\hat{l}_m,n}$ vanish on all sides $\hat{l}_s$, with $s \neq m$.
- $(k-1)^2$ internal functions $\hat{\varphi}^{\hat{K},n_0,n_1}$, with $0 \leq n_0, n_1 \leq k-2$

$$\hat{\varphi}^{\hat{K},n_0,n_1}(\xi_0,\xi_1) = \hat{\varphi}^{\hat{a}_0}(\xi_0,\xi_1)\hat{\varphi}^{\hat{a}_2}(\xi_0,\xi_1)f_{n_0}(\xi_0)f_{n_1}(\xi_1).$$

  These functions vanish at all sides and vertices.

Triangular case

A hierarchical polynomial basis for $\mathcal{P}_k = \mathcal{P}_k(\hat{K})$, of dimension $(k^2+3k+2)/2$ is formed by:

- 3 vertex functions $\hat{\varphi}^{\hat{a}_m}$

$$\hat{\varphi}^{\hat{a}_0}(\xi_0,\xi_1) = 1-\xi_0-\xi_1,$$
$$\hat{\varphi}^{\hat{a}_1}(\xi_0,\xi_1) = \xi_0,$$
$$\hat{\varphi}^{\hat{a}_2}(\xi_0,\xi_1) = \xi_1,$$

  such that $\hat{\varphi}^{\hat{a}_m}(\hat{a}_s) = \delta_{ms}$, and vanishing on the edge that does not share the vertex $\hat{a}_m$.
- if $k \geq 2$, one has $3(k-1)$ edge functions $\hat{\varphi}^{\hat{l}_m,n}$, $n = 0, 1, \ldots, k-2$

$$\hat{\varphi}^{\hat{l}_0,n}(\xi_0,\xi_1) = \hat{\varphi}^{\hat{a}_0}(\xi_0,\xi_1)\hat{\varphi}^{\hat{a}_1}(\xi_0,\xi_1)f_n(\xi_1+2\xi_0-1),$$
$$\hat{\varphi}^{\hat{l}_1,n}(\xi_0,\xi_1) = \hat{\varphi}^{\hat{a}_1}(\xi_0,\xi_1)\hat{\varphi}^{\hat{a}_2}(\xi_0,\xi_1)f_n(\xi_1-\xi_0),$$
$$\hat{\varphi}^{\hat{l}_2,n}(\xi_0,\xi_1) = \hat{\varphi}^{\hat{a}_2}(\xi_0,\xi_1)\hat{\varphi}^{\hat{a}_0}(\xi_0,\xi_1)f_n(1-\xi_0-2\xi_1).$$

  The edge functions $\hat{\varphi}^{\hat{l}_m,n}$ vanish on all sides $\hat{l}_s$, with $s \neq m$.
- $\frac{1}{2}(k-2)(k-1)$ internal functions $\hat{\varphi}^{\hat{K},n_0,n_1}$, $k \geq 3$, $0 \leq n_0+n_1 \leq k-3$

$$\hat{\varphi}^{\hat{K},n_0,n_1}(\xi_0,\xi_1) = \hat{\varphi}^{\hat{a}_0}(\xi_0,\xi_1)\hat{\varphi}^{\hat{a}_1}(\xi_0,\xi_1)\hat{\varphi}^{\hat{a}_2}(\xi_0,\xi_1)f_{n_0}(2\xi_0-1)f_{n_1}(2\xi_1-1),$$

  that vanish at all sides and vertices.

Table 1
Constant vector fields for quadrilateral and triangular master elements.

Quadrilateral case			Triangular case		
Edge fields					
$\mathbf{b}^{\hat{l}_0,\hat{a}_0}$	$\mathbf{b}^{\hat{l}_0,\hat{a}_1}$	$\mathbf{b}^{\hat{l}_0,\perp}$	$\mathbf{b}^{\hat{l}_0,\hat{a}_0}$	$\mathbf{b}^{\hat{l}_0,\hat{a}_1}$	$\mathbf{b}^{\hat{l}_0,\perp}$
$(0,-1)$	$(0,-1)$	$(0,-1)$	$(0,-1)$	$(1,-1)$	$(0,-1)$
$\mathbf{b}^{\hat{l}_1,\hat{a}_1}$	$\mathbf{b}^{\hat{l}_1,\hat{a}_2}$	$\mathbf{b}^{\hat{l}_1,\perp}$	$\mathbf{b}^{\hat{l}_1,\hat{a}_1}$	$\mathbf{b}^{\hat{l}_1,\hat{a}_2}$	$\mathbf{b}^{\hat{l}_1,\perp}$
$(1,0)$	$(1,0)$	$(1,0)$	$(1,0)$	$(0,1)$	$\left(\frac{1}{\sqrt{2}},\frac{1}{\sqrt{2}}\right)$
$\mathbf{b}^{\hat{l}_2,\hat{a}_2}$	$\mathbf{b}^{\hat{l}_2,\hat{a}_3}$	$\mathbf{b}^{\hat{l}_2,\perp}$	$\mathbf{b}^{\hat{l}_2,\hat{a}_2}$	$\mathbf{b}^{\hat{l}_2,\hat{a}_0}$	$\mathbf{b}^{\hat{l}_2,\perp}$
$(0,1)$	$(0,1)$	$(0,1)$	$(-1,1)$	$(-1,0)$	$(-1,0)$
$\mathbf{b}^{\hat{l}_3,\hat{a}_3}$	$\mathbf{b}^{\hat{l}_3,\hat{a}_0}$	$\mathbf{b}^{\hat{l}_3,\perp}$			
$(-1,0)$	$(-1,0)$	$(-1,0)$			
Internal fields					
$\mathbf{b}^{\hat{l}_0,\top}$	$\mathbf{b}^{\hat{l}_1,\top}$	$\mathbf{b}^{\hat{l}_2,\top}$	$\mathbf{b}^{\hat{l}_0,\top}$	$\mathbf{b}^{\hat{l}_1,\top}$	$\mathbf{b}^{\hat{l}_2,\top}$
$(1,0)$	$(0,1)$	$(-1,0)$	$(1,0)$	$(-1,1)$	$(0,-1)$
$\mathbf{b}^{\hat{l}_3,\top}$	$\mathbf{b}^{\hat{K}}_{(1)}$	$\mathbf{b}^{\hat{K}}_{(2)}$	$\mathbf{b}^{\hat{K}}_{(1)}$	$\mathbf{b}^{\hat{K}}_{(2)}$	
$(0,-1)$	$(1,0)$	$(0,1)$	$(1,0)$	$(0,1)$	

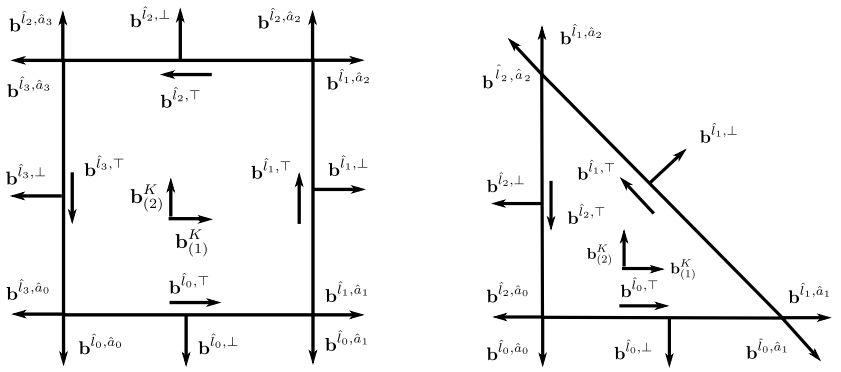

Fig. 3.2. Directions of the constant vector fields for the quadrilateral and triangular master elements.

3.3. Constant vector fields $\hat{\mathbf{b}}$ at the master element

To each basic element of $\hat{K}$ there are associated two constant and linearly independent vector fields:

- With every vertex $\hat{a}_s \in \hat{\mathcal{V}}$, there are associated fields $\hat{\mathbf{b}} = \mathbf{b}^{\hat{l}_m,\hat{a}_s}$, where $\hat{l}_m$ is an edge that has $\hat{a}_s$ as a vertex. Each $\mathbf{b}^{\hat{l}_m,\hat{a}_s}$ is aligned to the adjacent edge (which also shares $\hat{a}_s$ as a vertex) and has unitary component along the unitary external normal $\hat{\mathbf{n}}$ on the edge $\hat{l}_m$.
- With every edge $\hat{l}_s \in \hat{\mathcal{A}}$, there are associated the fields $\hat{\mathbf{b}} = \mathbf{b}^{\hat{l}_s,\top}$, aligned with the edge $\hat{l}_s$, and $\hat{\mathbf{b}} = \mathbf{b}^{\hat{l}_s,\perp}$ is the unitary external normal $\hat{\mathbf{n}}$ at $\hat{l}_s$.
- With the volume $\hat{K}$, there are associated fields $\hat{\mathbf{b}} = \mathbf{b}^{\hat{K}}_{(j)} = \mathbf{e}_{(j)}, j = 1, 2$.

These fields are grouped into two categories

1. Edge vector fields, incident with the edges $\hat{l}_m \in \hat{\mathcal{A}}$:
   (a) $\hat{\mathbf{b}} = \mathbf{b}^{\hat{l}_m,\hat{a}_s}$, associated with each vertex $\hat{a}_s \in \hat{\mathcal{V}}_m$.
   (b) $\hat{\mathbf{b}} = \mathbf{b}^{\hat{l}_m,\perp}$ associated with the edge $\hat{l}_m$.
2. Internal vector fields:
   (a) $\mathbf{b}^{\hat{l}_m,\top}$ aligned with the edge $\hat{l}_m$.
   (b) $\hat{\mathbf{b}} = \mathbf{b}^{\hat{K}}_{(j)} = \mathbf{e}_{(j)}, j = 1, 2$, associated to the interior of $\hat{K}$.

The constant vector fields $\hat{\mathbf{b}}$ associated with quadrilateral and triangular master elements detailed in Table 1, and their directions are illustrated in Fig. 3.2. Note that, in this figure, the shown vectors do not have the correct magnitude of the vector fields $\hat{\mathbf{b}}$.

3.4. Geometric mapping

Let $\mathbf{x} : \mathbb{R}^2 \to \mathbb{R}^d,\ d = 2, 3$ be a regular geometric mapping (at least C^1). The geometric mappings implemented in NeoPZ are described in [16] using the transfinite interpolation methodology [17].

Let $\mathbf{x} = (x_j),\ j = 1, \ldots, d$, and $\mathbf{J} = \nabla\mathbf{x}$ the Jacobian matrix of this mapping, that is

$$\mathbf{J} = [\boldsymbol{\partial}_0\ \boldsymbol{\partial}_1] = \begin{bmatrix} \frac{\partial x_0}{\partial \xi_0} & \frac{\partial x_0}{\partial \xi_1} \\ \frac{\partial x_1}{\partial \xi_0} & \frac{\partial x_1}{\partial \xi_1} \end{bmatrix} \quad \text{or} \quad \mathbf{J} = [\boldsymbol{\partial}_0\ \boldsymbol{\partial}_1] = \begin{bmatrix} \frac{\partial x_0}{\partial \xi_0} & \frac{\partial x_0}{\partial \xi_1} \\ \frac{\partial x_1}{\partial \xi_0} & \frac{\partial x_1}{\partial \xi_1} \\ \frac{\partial x_2}{\partial \xi_0} & \frac{\partial x_2}{\partial \xi_1} \end{bmatrix},$$

where the columns are given by $\boldsymbol{\partial}_i = (\frac{\partial \mathbf{x}}{\partial \xi_i})$. In the finite element method, it is assumed that $\mathbf{x}$ is a diffeomorphism between the elements $\hat{K}$ and K (i.e., $\mathbf{x} : \hat{K} \to K$ is a bijection with differentiable inverse $\mathbf{x}^{-1}$). For this purpose, the columns $\boldsymbol{\partial}_i$ of $\mathbf{J}$ must be linearly independent. The determinant (or pseudo-determinant) $\det\ \mathbf{J}$ of the Jacobian matrix is defined as the area of the parallelogram generated by the two columns of $\mathbf{J}$, i.e.,

$$\det\ \mathbf{J} = \|\boldsymbol{\partial}_0 \times \boldsymbol{\partial}_1\|, \tag{3.1}$$

where $\|\mathbf{v}\| = \sqrt{\langle \mathbf{v}, \mathbf{v}\rangle}$ denotes Euclidean norm in $\mathbb{R}^d$ derived from the inner product $\langle , \rangle$.

Let α be the angle formed by $\boldsymbol{\partial}_0$ and $\boldsymbol{\partial}_1$. Since $\langle \boldsymbol{\partial}_0, \boldsymbol{\partial}_1\rangle = \|\boldsymbol{\partial}_0\|\ \|\boldsymbol{\partial}_1\| \cos\alpha$ and $\|\boldsymbol{\partial}_0 \times \boldsymbol{\partial}_1\| = \|\boldsymbol{\partial}_0\|\ \|\boldsymbol{\partial}_1\| \sin\alpha$, it results that $\langle \boldsymbol{\partial}_0, \boldsymbol{\partial}_1\rangle^2 + \|\boldsymbol{\partial}_0 \times \boldsymbol{\partial}_1\|^2 = \|\boldsymbol{\partial}_0\|^2\ \|\boldsymbol{\partial}_1\|^2$. Then, it follows that

$$\det\ \mathbf{J} = \|\boldsymbol{\partial}_0 \times \boldsymbol{\partial}_1\| = \sqrt{\|\boldsymbol{\partial}_0\|^2\ \|\boldsymbol{\partial}_1\|^2 - \langle \boldsymbol{\partial}_0, \boldsymbol{\partial}_1\rangle} = \sqrt{\det\ \mathbf{G}},$$

where the matrix $\mathbf{G} = \mathbf{J}^t\mathbf{J} = (g_{i,j})$ has coordinates $g_{i,j} = \langle \boldsymbol{\partial}_i, \boldsymbol{\partial}_j\rangle$.

Tangent plane

Let $T_{\mathbf{p}}(K) \subset \mathbb{R}^d$ be the tangent plane to K at the point $\mathbf{p} = \mathbf{x}(\boldsymbol{\xi})$. It is generated by the columns of the Jacobian matrix. Precisely, if $\mathbf{v} \in T_{\mathbf{p}}(K)$, then $\mathbf{v} = \sum v_i\boldsymbol{\partial}_i = \mathbf{J}\hat{\mathbf{v}}$, where $\hat{\mathbf{v}} = (v_i) \in \mathbb{R}^2$. For planar elements $K \subset \mathbb{R}^2$, the tangent plane is the Euclidean space $\mathbb{R}^2$.

It can be observed that for $\mathbf{w} = \mathbf{J}\hat{\mathbf{w}} = \sum w_i\boldsymbol{\partial}_i,\ \mathbf{v} = \mathbf{J}\hat{\mathbf{v}} = \sum_i v_i\boldsymbol{\partial}_i \in T_{\mathbf{p}}(K)$,

$$\langle \mathbf{v}, \mathbf{w}\rangle = [\mathbf{J}\hat{\mathbf{v}}]^t[\mathbf{J}\hat{\mathbf{w}}] = [\hat{\mathbf{v}}^t\mathbf{J}^t][\mathbf{J}\hat{\mathbf{w}}] = \hat{\mathbf{v}}^t\mathbf{J}^t\mathbf{J}\hat{\mathbf{w}} = \hat{\mathbf{v}}^t\mathbf{G}\hat{\mathbf{w}}.$$

4. H^1-conforming spaces based on curved meshes

In the present section, the main aspects for the construction of H^1-conforming spaces based on curved meshes over manifolds immersed in $\mathbb{R}^3$ are described. The procedure is similar to the ones used for regions in linear Euclidean geometries, but some specific tools from calculus on manifolds are required. The content refers to Items 4 and 5 of the Script section.

4.1. Transformation of scalar functions $\varphi = \mathbb{F}\hat{\varphi}$

The scalar functions defined in the master element $\hat{K}$ may be mapped to functions defined in K by the operator $\varphi = \mathbb{F}\hat{\varphi}$ defined by the composition

$$\varphi = \hat{\varphi} \circ \mathbf{x}^{-1}.$$

In the case of mappings between spaces of same dimension (i.e., $d = 2$), the classic formulae for the change of variables in integrals are

$$\int_K \mathbb{F}\hat{\varphi}\, dS = \int_{\hat{K}} \hat{\varphi}\ \det\ \mathbf{J} d\boldsymbol{\xi},$$
$$\int_{\partial K} \mathbb{F}\hat{\varphi}\, ds = \int_{\partial\hat{K}} \hat{\varphi}\mathbf{J}_{\hat{\mathbf{n}}} d\hat{s},$$

where $\mathbf{J}_{\hat{\mathbf{n}}} = \det\ \mathbf{J}\ \|(\mathbf{J}^{-1})^t\hat{\mathbf{n}}\|$. For mappings to an immersed manifold in higher dimensional space (i.e., $d = 3$), these formulae are valid with $\mathbf{J}_{\hat{\mathbf{n}}} = \det\ \mathbf{J}\ \|(\mathbf{J}^{\dagger})^t\hat{\mathbf{n}}\|$, where $\mathbf{J}^{\dagger} = (\mathbf{J}^t\mathbf{J})^{-1}\mathbf{J}^t$ is the pseudo-inverse of the Jacobian matrix $\mathbf{J}$. It is observed that in the case of Euclidean elements of the same dimension, $\mathbf{J}$ is a square matrix and $\mathbf{J}^{\dagger} = \mathbf{J}^{-1}\mathbf{J}^{-t}\mathbf{J}^t = \mathbf{J}^{-1}$, recovering the standard formulae for $d = 2$.

Gradient operator

For a mapping between Euclidean spaces of the same dimension (e.g. see [1]), the gradient is given by

$$\nabla\varphi = (\mathbf{J}^{-1})^t\hat{\nabla}\hat{\varphi}. \tag{4.1}$$

In the case of mapping onto a manifold K immersed in $\mathbb{R}^3$, the gradient $\nabla_K\varphi$ of a scalar function $\varphi : K \to \mathbb{R}$ is an operator defined on $T_{\mathbf{p}}(K)$, for each point $\mathbf{p} \in K$, so that for $\mathbf{v} \in T_{\mathbf{p}}(K)$

$$\langle \nabla_K\varphi, \mathbf{v}\rangle = d\varphi(\mathbf{v}).$$

For transformed scalar functions $\varphi = \mathbb{F}\hat{\varphi} = \hat{\varphi} \circ \mathbf{x}^{-1}$, and $\mathbf{v} = \sum_i v_i \boldsymbol{\partial}_i$, then

$$d\varphi(\mathbf{v}) = \sum v_i d\varphi(\boldsymbol{\partial}_i) = \sum v_i \frac{\partial\hat{\varphi}}{\partial\xi_i}.$$

Combining these two expressions with the representation $\nabla_K\varphi = \sum_i \alpha_i \boldsymbol{\partial}_i$, then

$$d\varphi(\mathbf{v}) = \langle \nabla_K\varphi, \mathbf{v}\rangle = \sum_{i,j} g_{i,j}.v_i.\alpha_j = \sum v_i \frac{\partial\hat{\varphi}}{\partial\xi_i},$$

from which it follows that

$$\sum_j g_{i,j}.\alpha_j = \frac{\partial\hat{\varphi}}{\partial\xi_i}, \quad \forall i.$$

That is, if $\boldsymbol{\alpha} = (\alpha_i)$, then $\mathbf{G}\alpha = \nabla\hat{\varphi}$, which means that $\alpha = \mathbf{G}^{-1}\nabla\hat{\varphi}$. That is, if $G^{-1} = (g^{i,j})$, then

$$\nabla_K\varphi(\mathbf{x}(\boldsymbol{\xi})) = \sum_{i,j} g^{i,j}(\boldsymbol{\xi}) \frac{\partial\hat{\varphi}(\boldsymbol{\xi})}{\partial\xi_{\mathbf{j}}} \frac{\partial\mathbf{x}(\boldsymbol{\xi})}{\partial\xi_{\mathbf{i}}}. \tag{4.2}$$

Another way to express this formula is given by

$$\nabla_K\varphi = (\mathbf{J}^{\dagger})^t \nabla\hat{\varphi}. \tag{4.3}$$

It can be observed that in the case of elements in Euclidean spaces of the same dimension, in which $\mathbf{J}^{\dagger} = \mathbf{J}^{-1}$, the formula (4.1) is recovered.

4.2. H^1-conforming subspaces

For regions $\Omega \subset \mathbb{R}^d$, consider the Sobolev space

$$H^1(\Omega) = \left\{u \in L^2(\Omega);\ \nabla u \in [L^2(\Omega)]^d\right\},$$

with the norm

$$\|u\|_{H^1} = [\|u\|^2_{L^2} + \|\nabla u\|^2_{L^2}]^{1/2},$$

and denote by $H^{1/2}(\partial\Omega)$ the trace space $u|_{\partial\Omega}$ of functions $u \in H^1(\Omega)$.

Let $u \in H^1(\Omega)$, Γ a partition of Ω, and K^ℓ, $K^j \in \Gamma$ be two neighboring elements sharing a common edge $l^{\ell,j} = K^\ell \cap K^j$. Let $u^{K^\ell} = u|_{K^\ell} \in H^1(K^\ell)$ and $u^{K^j} = u|_{K^j} \in H^1(K^j)$. Suppose a fixed direction η is determined by the external normal of K^ℓ at $l^{\ell,j}$. Define the trace jump of u at the interface $l^{\ell,j}$ (in the sense of $H^{1/2}$) as

$$[\![u]\!]|_{l^{\ell,j}} = u^{K^j}|_{l^{\ell,j}} - u^{K^\ell}|_{l^{\ell,j}}. \tag{4.4}$$

Theorem 4.1 (*Characterization of $H^1(\Omega)$*)**.** *A function $u \in L^2(\Omega)$ is in $H^1(\Omega)$ if and only if, to each element K in a partition of Ω, the following properties are valid:* (a) $u^K = u|_K \in H^1(K)$*;* (b) *the trace jump of u at interfaces of the elements is zero.*

Scalar shape functions in $H^1(K)$

Using the transformation $\mathbb{F}$, the hierarchical polynomial basis $\hat{\mathcal{B}}_k$ of $\mathcal{P}_k$ is mapped onto a basis $\mathcal{B}_k^K$ for a finite element subspace in $H^1(K)$. Thus, the basic functions in $\mathcal{B}_k^K$ are classified as:

- **Vertex functions**: $\varphi^{a_m}(\mathbf{p}) = \mathbb{F}[\hat{\varphi}^{\hat{a}_m}(\tilde{\boldsymbol{\xi}})]$, such that $\varphi^{a_m}(a_s) = \delta_{ms}$, that vanish at all edges of K that does not share a_m.
- **Edge functions**: $\varphi^{l_m,n}(\mathbf{p}) = \mathbb{F}[\hat{\varphi}^{\hat{l}_m,n}(\tilde{\boldsymbol{\xi}})]$, and vanish at all edges l_s, with $s \neq m$ (and all vertices).
- **Internal functions** $\varphi^{K,n_1,n_2}(\mathbf{p}) = \mathbb{F}[\hat{\varphi}^{\hat{K},n_1,n_2}(\tilde{\boldsymbol{\xi}})]$, that vanish at all edges and vertices of K.

In this definition, the notation $\tilde{\boldsymbol{\xi}}$ corresponds to an appropriate parametrization of $\hat{K}$ which ensures continuity of the bases at the interface between the elements of the partition.

This set of vertex, edge and internal functions is linearly independent, forming a basis for a subspace of $H^1(K)$

$$\mathcal{B}_k^K = \left\{\varphi^{a_m},\ \varphi^{l_m,n},\ \varphi^{K,n_1,n_2}\right\}. \tag{4.5}$$

Global continuity for subspaces of $H^1(\Omega)$

We consider the subspace V_k^Γ of scalar functions u defined by parts, such that $u^K = u|_K \in \text{span } \mathcal{B}_k^K \subset H^1(K)$. Let K^ℓ, $K^j \in \Gamma$ be two neighboring elements sharing a common edge $l^{\ell,j} = K^\ell \cap K^j$, $u^{K^\ell} = u|_{K^\ell} \in \text{span } \mathcal{B}_k^{K^\ell}$ and $u^{K^j} = u|_{K^j} \in \text{span } \mathcal{B}_k^{K^j}$. In order for a function $u \in V_k^\Gamma$ to be in $H^1(\Omega)$, the zero jump property $u^{K^j}|_{l^{\ell,j}} - u^{K^\ell}|_{l^{\ell,j}} = 0$ at the interface $l^{\ell,j}$ must be verified. For this, the coefficients of the vertex and edge functions in the expansion of u^{K^ℓ} in terms of the basis $\mathcal{B}_k^{K^\ell}$ must be linked to those of the expansion of u^{K^j} in the neighboring element K^j. The coefficients of the internal basic functions need not to be linked, since the internal functions vanish at all edges and do not affect the continuity of u at interfaces. The same fact applies to vertex functions φ^{a_m} for vertices outside $l^{\ell,j}$, and for edge functions φ^{l_m} with $l_m \neq l^{\ell,j}$, since they also vanish in $l^{\ell,j}$, not contributing to the jump trace of u at this interface. But the vertex functions associated with the vertices of the edge $l^{\ell,j}$ and edge functions associated with $l^{\ell,j}$ itself do contribute to the jump trace at this interface. However, as described in [13], the appropriate choice of parametrization $\tilde{\boldsymbol{\xi}}$ for the master element allows the jump of these basic functions to be zero at the interface. Thus, to ensure zero jump trace of u, it is sufficient to assure that the coefficients of the vertex functions associated with the vertices of $l^{\ell,j}$ and the edge shape functions associated to the edge $l^{\ell,j}$ are coincident in both elements sharing the interface. This result is summarized in the following theorem.

Theorem 4.2. *Let Γ be a partition of the domain Ω in elements K mapped from triangular or quadrilateral master elements. Consider hierarchical bases $\mathcal{B}_k^K$ for subspaces in $H^1(K)$ as stated in (4.5). Let V_k^Γ be the subspace of scalar functions u such that $u^K = u|_K \in$ span $\mathcal{B}_k^K \subset H^1(K)$. Suppose that in the expansions of u^{K^ℓ} and u^{K^j}, with respect to the bases $\mathcal{B}_k^{K^\ell}$ and $\mathcal{B}_k^{K^j}$ of two neighboring elements $K^\ell, K^j \in \Gamma$ sharing a common edge $l^{\ell,j} = K^\ell \cap K^j$ the corresponding coefficients multiplying vertex and edge shape functions associated to the common interface are identical. Then the space V_k^Γ is a H^1-conforming finite element space.*

5. H(div)-conforming spaces based on curved elements

The present section concerns with the construction of $\mathbf{H}(\text{div})$-conforming spaces based on curved meshes of manifolds immersed in $\mathbb{R}^3$, the main topic of this paper. The content refers to Items 6, 7 and 8 of the Script section. Some specific tools and properties of the divergence operator, and Piola transformation on manifolds are required. Through this text, the notation $\mathbf{n}$ refers to a unitary external normal to a region, and, if necessary, $\mathbf{n}^K$ is used to identify the specific region K.

5.1. Properties related to the divergence operator

The divergent operator $\nabla \cdot \boldsymbol{\Phi}$ converts a vector field $\boldsymbol{\Phi} : \mathbf{p} \in \Omega \to \boldsymbol{\Phi}(\mathbf{p}) \in T_{\mathbf{p}}(\Omega)$ into a scalar function. Conceptually, it is defined as

$$\nabla \cdot \boldsymbol{\Phi}(\mathbf{p}) = \lim_{K \to \{\mathbf{p}\}} \frac{1}{|K|} \int_{\partial K} \langle \boldsymbol{\Phi}, \mathbf{n} \rangle ds.$$

For vector fields defined on a manifold $\boldsymbol{\Phi} : \Omega \to T_{\mathbf{p}}(\Omega)$, with representation $\boldsymbol{\Phi} = \sum_i \Phi_i \boldsymbol{\partial}_i$, the divergence representation in local coordinates is given by

$$\nabla \cdot \boldsymbol{\Phi} = \mathbb{F}\left[\frac{1}{\det \mathbf{J}} \sum_i \frac{\partial}{\partial \xi_i} ((\Phi_i \circ \mathbf{x}) \ \det \mathbf{J}) \right]. \tag{5.1}$$

The space $\mathbf{H}(\text{div}, \Omega)$ is defined by

$$\mathbf{H}(\text{div}, \Omega) = \left\{ \boldsymbol{\Phi} : \Omega \to T_{\mathbf{p}}(\Omega);\ \boldsymbol{\Phi} \in [L^2(\Omega)]^d;\ \text{and } \nabla \cdot \boldsymbol{\Phi} \in L^2(\Omega) \right\},$$

with the norm

$$\|\boldsymbol{\Phi}\|_{\mathbf{H}(\text{div})} = \left[\|\boldsymbol{\Phi}\|_{L^2}^2 + \|\nabla \cdot \boldsymbol{\Phi}\|_{L^2}^2 \right]^{1/2}.$$

For functions $\boldsymbol{\Phi} \in \mathbf{H}(\text{div}, \Omega)$, consider the normal component $\langle \boldsymbol{\Phi}, \mathbf{n} \rangle \in H^{-1/2}(\partial\Omega)$, where $H^{-1/2}(\partial\Omega)$ is the dual space of $H^{1/2}(\partial\Omega)$ and $\mathbf{n}$ is the unit outward normal over $\partial\Omega$.

Theorem 5.1 (*Green's Formula [2]*)**.** *For scalar functions $\varphi : \Omega \to \mathbb{R}$ in $H^1(\Omega)$ and vectorial functions $\boldsymbol{\Phi} : \Omega \to T_{\mathbf{p}}(\Omega)$ in $\mathbf{H}(\text{div}, \Omega)$ the integration by parts formula is valid*

$$\int_\Omega \langle \nabla \varphi, \boldsymbol{\Phi} \rangle dS = -\int_\Omega \varphi \ \text{div } \boldsymbol{\Phi} dS + \int_{\partial\Omega} \varphi \langle \boldsymbol{\Phi}, \mathbf{n} \rangle ds. \tag{5.2}$$

Let $\boldsymbol{\Phi} : \Omega \to T_{\mathbf{p}}(\Omega)$ be a vectorial function, and consider $K^\ell, K^j \in \Gamma$ be two neighboring elements sharing a common edge $l^{\ell,j} = K^\ell \cap K^j$, with exterior unit normal $\mathbf{n}^{K^\ell}$ and $\mathbf{n}^{K^j}$, respectively. Being $\boldsymbol{\Phi}^{K^\ell} = \boldsymbol{\Phi}|_{K^\ell} \in \mathbf{H}(\mathrm{div}, K^\ell)$ and $\boldsymbol{\Phi}^{K^j} = \boldsymbol{\Phi}|_{K^j} \in \mathbf{H}(\mathrm{div}, K^j)$, define the jump of the normal component at the interface $l^{\ell,j}$ (in the sense of $H^{-1/2}(\partial K)$) by

$$[\![\boldsymbol{\Phi}]\!] = \langle \boldsymbol{\Phi}^{K^j}, \mathbf{n}^{K^j} \rangle|_{l^{\ell,j}} + \langle \boldsymbol{\Phi}^{K^\ell}, \mathbf{n}^{K^\ell} \rangle|_{l^{\ell,j}}. \tag{5.3}$$

Theorem 5.2 (*Characterization of* $\mathbf{H}(\mathrm{div}, \Omega)$). *A vector field* $\boldsymbol{\Phi} : \Omega \to T_{\mathbf{p}}(\Omega) \in [L^2(\Omega)]^d$ *is in* $\mathbf{H}(\mathrm{div}, \Omega)$ *if and only if given any partition* Γ*:* (a) *for all element* $K \in \Gamma$, $\boldsymbol{\Phi}^K = \Phi|_K \in \mathbf{H}(\mathrm{div}, K)$*;* (b) *the jump of the normal component at element interfaces is zero.*

In the case of regions $\Omega \subset \mathbb{R}^2$, the result is known in the literature [1]. The proof for the case of manifolds immersed in $\mathbb{R}^3$ is similar, and it is based on the Green's formula (5.2).

5.2. Piola transformation of vector fields $\boldsymbol{\Phi} = \mathbb{F}^{\mathrm{div}}\hat{\boldsymbol{\Phi}}$

Let $\mathbf{x} : \hat{K} \to K$ be a regular geometric mapping. In building a subspace of $\mathbf{H}(\mathrm{div}, K)$ by the transformation of vector fields in $\mathbf{H}(\mathrm{div}, \hat{K})$, the operator $\mathbb{F}$ does not apply, since it cannot preserve normal components, not even mapping $\mathbf{H}(\mathrm{div}, \hat{K})$ on $\mathbf{H}(\mathrm{div}, K)$. For this, the contravariant Piola transformation $\mathbb{F}^{\mathrm{div}} : \hat{\boldsymbol{\Phi}} \to \boldsymbol{\Phi}$, associated with the geometric mapping $\mathbf{x}$, is used to relate vectorial functions $\hat{\boldsymbol{\Phi}}$ defined in the master element $\hat{K}$ with vectorial functions $\boldsymbol{\Phi}$ defined in geometrical elements K by the formula

$$\boldsymbol{\Phi} = \mathbb{F}\left[\frac{1}{\det \mathbf{J}}\mathbf{J}\hat{\boldsymbol{\Phi}}\right]. \tag{5.4}$$

As reported in [1], for a mapping between Euclidean spaces of the same dimension, divergence of vectorial fields given by the Piola contravariant transformation verifies the expression

$$\nabla.\boldsymbol{\Phi} = \mathbb{F}\left[\frac{1}{\det \mathbf{J}}\hat{\nabla} \cdot \hat{\boldsymbol{\Phi}}\right]. \tag{5.5}$$

Furthermore, if $\varphi = \mathbb{F}\hat{\varphi}$, the following identities are valid

$$\int_K \langle \boldsymbol{\Phi}, \nabla\varphi \rangle \, d\mathbf{p} = \int_{\hat{K}} \langle \hat{\boldsymbol{\Phi}}, \hat{\nabla}\hat{\varphi} \rangle \, d\boldsymbol{\xi}, \tag{5.6}$$

$$\int_K \varphi \, \nabla.\boldsymbol{\Phi} \, d\mathbf{p} = \int_{\hat{K}} \hat{\varphi} \, \hat{\nabla}.\hat{\boldsymbol{\Phi}} d\boldsymbol{\xi}, \tag{5.7}$$

$$\int_{\partial K} \langle \boldsymbol{\Phi}, \mathbf{n} \rangle \varphi \, d\sigma = \int_{\partial \hat{K}} \langle \hat{\boldsymbol{\Phi}}, \hat{\mathbf{n}} \rangle \hat{\varphi} \, d\hat{s}. \tag{5.8}$$

As a result, $\mathbb{F}^{\mathrm{div}}$ is an isomorphism between $\mathbf{H}(\mathrm{div}, \hat{K})$ and $\mathbf{H}(\mathrm{div}, K)$, preserving normal components, in the $H^{-1/2}$ sense. These results can be extended to manifolds, as stated in the next theorem. See also [4].

Theorem 5.3. *Let vector fields* $\boldsymbol{\Phi}$ *in* K *and* $\hat{\boldsymbol{\Phi}}$ *in* $\hat{K}$ *be related by Piola transformation* (5.4)*, and consider* $\varphi = \mathbb{F}\hat{\varphi}$*. Then the formula* (5.5) *and identities* (5.6)–(5.8) *are valid. Consequently,* $\mathbb{F}^{\mathrm{div}}$ *defines an isomorphism between* $\mathbf{H}(\mathrm{div}, \hat{K})$ *and* $\mathbf{H}(\mathrm{div}, K)$*, preserving the normal traces of the fields on the boundary of the elements in the sense of* $H^{-1/2}$.

5.3. Vector fields on the geometric element K

As stated in Section 2, the construction of fields $\mathbf{v}$ on a curved element K begins with the definition of vector fields $\mathbf{b}$ obtained from the Piola mapping $\mathbb{F}^{\mathrm{div}}\hat{\mathbf{b}}$ of constant vector fields $\hat{\mathbf{b}}$, defined in the master element, as stated in Section 3.3. The next step is a normalization procedure, which is applied in order to ensure unitary normal component of edge fields on their associated edges. Interior fields do not require such normalization because their normal components vanish at all element edges.

Piola transformation of fields $\hat{\mathbf{b}}$

From the constant vector fields $\hat{\mathbf{b}}$ defined over the master element, and using the Piola transformation $\mathbb{F}^{\mathrm{div}}$, fields $\mathbf{b}$ are defined in K. That is,

$$\mathbf{b} = \mathbb{F}^{\mathrm{div}}\hat{\mathbf{b}} = \frac{1}{\det \mathbf{J}}\mathbf{J}\hat{\mathbf{b}}.$$

Following the classification of the original fields $\hat{\mathbf{b}}$, they are also classified as edge and internal fields. The vertices and edges of K are defined by geometric mapping of the respective sub-elements in the master element $\hat{K}$: $a_m = \mathbf{x}(\hat{a}_m)$ and $l_m = \mathbf{x}(\hat{l}_m)$.

Normalization of the edge fields

For each edge $\hat{l}$ of $\hat{K}$ and each edge vector field $\hat{\mathbf{b}}$, a constant vector field $\hat{\mathbf{t}}$ tangent to $\hat{l} \in \hat{\mathcal{A}}$ is considered, such that the pair $\{\hat{\mathbf{n}}, \hat{\mathbf{t}}\}$ is positively oriented, and $\|\hat{\mathbf{t}} \times \hat{\mathbf{b}}\| = 1$. Therefore,

$$\det \mathbf{J} = \frac{\|\mathbf{J}\,\hat{\mathbf{t}} \times \mathbf{J}\,\hat{\mathbf{b}}\|}{\|\hat{\mathbf{t}} \times \hat{\mathbf{b}}\|} = \|\mathbf{J}\,\hat{\mathbf{t}}\|\ \|\mathbf{J}\,\hat{\mathbf{b}}\|\ \sin\theta,$$

where θ is the angle between $\mathbf{J}\,\hat{\mathbf{t}}$ and $\mathbf{J}\,\hat{\mathbf{b}}$, with $0 \leq \theta \leq \pi$. To edge fields $\mathbf{b} = \mathbb{F}^{\text{div}}\hat{\mathbf{b}}$, consider the normalized fields

$$\mathbf{v} = \mathbf{b}\|\mathbf{J}\hat{\mathbf{t}}\|$$

and the fields

$$\mathbf{n} = \frac{\left(\frac{\partial \mathbf{x}(\boldsymbol{\xi})}{\partial \xi_0} \times \frac{\partial \mathbf{x}(\boldsymbol{\xi})}{\partial \xi_1}\right) \times \mathbf{J}\hat{\mathbf{t}}}{\left\|\left(\frac{\partial \mathbf{x}(\boldsymbol{\xi})}{\partial \xi_0} \times \frac{\partial \mathbf{x}(\boldsymbol{\xi})}{\partial \xi_1}\right) \times \mathbf{J}\hat{\mathbf{t}}\right\|}.$$

As $\mathbf{J}\hat{\mathbf{t}}$ is contained in the tangent plane to K at the point $\mathbf{p} = \mathbf{x}(\boldsymbol{\xi})$, the same is true for $\mathbf{n}$, which is unitary and orthogonal to $\mathbf{J}\hat{\mathbf{t}}$. Regardless the magnitude of $\hat{\mathbf{t}}$, it is shown that $\mathbf{n} = \mathbf{n}^K$ is the unitary external normal to K at the edge $l = \mathbf{x}(\hat{l})$.

Proposition. *Let $l_m \in \mathcal{A}$ be an edge of K.*

(a) *The edge vector fields $\mathbf{v} = \mathbf{v}^{l_m, a_s}$ and $\mathbf{v} = \mathbf{v}^{l_m, \perp}$ have unitary normal component along l_m;*
(b) *the field $\mathbf{v} = \mathbf{v}^{l_m, \top}$ has zero normal component along l_m;*
(c) *if l is the adjacent edge to l_m at a vertex a_s, then the normal component of the field $\mathbf{v} = \mathbf{v}^{l, a_s}$ vanishes along l_m.*

Proof. The edge fields are defined by $\mathbf{v} = \frac{\|\mathbf{J}\hat{\mathbf{t}}\|}{\det \mathbf{J}}(\mathbf{J}\,\hat{\mathbf{b}})$, by applying the Piola transform in the fields $\hat{\mathbf{b}} = \mathbf{b}^{\hat{l}_m, \hat{a}_s}$ and $\hat{\mathbf{b}} = \mathbf{b}^{\hat{l}_m, \perp}$ and normalizing by $\|\mathbf{J}\hat{\mathbf{t}}\|$. Therefore, it follows that

$$\begin{aligned}\mathbf{v}.\mathbf{n} &= \frac{\|\mathbf{J}\hat{\mathbf{t}}\|}{\det \mathbf{J}}(\mathbf{J}\,\hat{\mathbf{b}}).\mathbf{n}_m \\ &= \frac{\|\mathbf{J}\hat{\mathbf{t}}\|}{\|\mathbf{J}\,\hat{\mathbf{t}}\|\ \|\mathbf{J}\,\hat{\mathbf{b}}\|\ \sin\theta}\|\mathbf{J}\,\hat{\mathbf{b}}\|\ \|\mathbf{n}_m\|\ \cos(\alpha),\end{aligned}$$

where α is the angle between $\mathbf{J}\,\hat{\mathbf{b}}$ and $\mathbf{n}$. Taking into account the orthogonality property $\mathbf{J}\hat{\mathbf{t}} \perp \mathbf{n}$, then $\alpha = \frac{\pi}{2} - \theta$ or $\alpha = \theta - \frac{\pi}{2}$, which leads to $\mathbf{v}.\mathbf{n} = 1$.

For the field $\mathbf{v} = \mathbf{v}^{l_m, \top} = \mathbb{F}^{\text{div}}\mathbf{b}^{\hat{l}_m, \top}$, obtained by the Piola transformation of the field $\hat{\mathbf{b}} = \mathbf{b}^{\hat{l}_m, \top}$, the component along the external normal $\mathbf{n}_m$ to the edge l_m is zero because $\mathbf{b}^{\hat{l}_m, \top}$ is tangent to $\hat{l}_m$ (and therefore orthogonal to $\hat{\mathbf{n}}_m$) and because the Piola transformation maintains the normal components of the fields.

If $l = \mathbf{x}(\hat{l})$ and $l_m = \mathbf{x}(\hat{l}_m)$ are adjacent edges in K, then $\hat{l}$ and $\hat{l}_m$ are also adjacent at the master element, sharing the vertex $\hat{a}_s$ (such that $a_s = \mathbf{x}(\hat{a}_s)$). The edge field $\mathbf{v} = \mathbf{v}^{l, a_s}$ is obtained by the normalization of the Piola transformation of the field $\hat{\mathbf{b}} = \mathbf{b}^{\hat{l}, \hat{a}_s}$. By definition, $\mathbf{b}^{\hat{l}, \hat{a}_s}$ is aligned with the adjacent edge $\hat{l}_m$, and hence having zero normal component over $\hat{l}_m$. Because the Piola transform preserves the normal components of the fields, it follows that the normal component of $\mathbf{v}^{l, a_s}$ is also zero over l_m. □

In summary, the fields $\mathbf{v}$ are classified as:

1. Edge fields, incident to the edges $l_m \in \mathcal{A}$:
   (a) for each vertex $a_s \in \mathcal{V}_m$, it is associated a vector field $\mathbf{v} = \mathbf{v}^{l_m, a_s}$, with unitary normal component over l_m. If l is an adjacent edge to l_m, sharing the vertex a_s, then the unit normal component of $\mathbf{v}^{l, a_s}$ over $\mathbf{n}_m$ is zero.
   (b) to every edge l_m, it is associated a vector field $\mathbf{v} = \mathbf{v}^{l_m, \perp}$, with unitary normal component over it.
2. Internal fields
   (a) for each edge $l_m \in \mathcal{A}$, it is associated a vector field $\mathbf{v} = \mathbf{v}^{l_m, \top}$, tangent to it (i.e., with zero normal component over l_m).
   (b) For the volume K, two linearly independent fields $\mathbf{v} = \mathbf{v}^K_{(j)}, j = 1, 2$ are associated.

5.4. Hierarchical vectorial bases for subspaces in $\mathbf{H}(\text{div}, K)$ and their properties

Let $\varphi = \mathbb{F}[\hat{\varphi}(\tilde{\boldsymbol{\xi}})]$ be scalar shape functions in $H^1(K)$, defined in (4.2). The interest is in the construction of vectorial shape functions $\boldsymbol{\Phi}$ in the geometric element K by multiplication

$$\boldsymbol{\Phi}(\mathbf{p}) = \varphi\mathbf{v},$$

where $\mathbf{v}$ is one of the fields obtained in Section 5.3, by Piola transformation applied to constant vector fields $\hat{\mathbf{b}}$ defined in the master element. The resulting hierarchical vectorial shape functions are organized according to the following classification:

- **Edge functions**:
  $\boldsymbol{\Phi}^{l_m,a_s}(\boldsymbol{p})$- multiplication of scalar functions $\varphi^{a_s}(\boldsymbol{p})$ associated to vertices $a_s \in \mathcal{V}_m$ with the corresponding edge vector fields $\mathbf{v}^{l_m,a_s}$.
  $\boldsymbol{\Phi}^{l_s,n}(\boldsymbol{p})$- multiplication of scalar functions $\varphi^{l_s,n}(\boldsymbol{p})$ associated to edges $l_s \in \mathcal{A}$ with the corresponding edge fields $\mathbf{v}^{l_s,\perp}$.
- **Internal functions**:
  $\boldsymbol{\Phi}^{K,l_m,n}(\boldsymbol{p})$- multiplication of scalar functions $\varphi^{l_m,n}(\boldsymbol{p})$ with vector fields $\mathbf{v}^{l_m,\top}$ aligned with such edges.
  $\boldsymbol{\Phi}^{K,n_1,n_2}_{(j)}(\boldsymbol{p})$- multiplication of scalar functions $\varphi^{K,n_1,n_2}(\boldsymbol{p})$ with vector fields $\mathbf{v}^K_{(j)}$, $j = 1, 2$, associated with the interior of K.

Let $\mathbf{B}^K_k$ be the set formed by these edge and internal functions

$$\mathbf{B}^K_k = \underbrace{\left\{\boldsymbol{\Phi}^{l_m,a_s}, \boldsymbol{\Phi}^{l_m,n}\right\}}_{\text{edge functions}} \bigcup \underbrace{\left\{\boldsymbol{\Phi}^{K,l_m,n}, \boldsymbol{\Phi}^{K,n_1,n_2}_{(1)}, \boldsymbol{\Phi}^{K,n_1,n_2}_{(2)}\right\}}_{\text{internal functions}}. \tag{5.9}$$

It is clear that span $\mathbf{B}^K_k \subset \mathbf{H}(\mathrm{div}, K)$. It can also be observed that each scalar function of the basis $\mathcal{B}^K_k$ appears twice in the composition of the vectorial shape functions in $\mathbf{B}^K_k$:

- **Vertex scalar functions**: the function φ^{a_s} appears in the composition of edge vectorial functions $\boldsymbol{\Phi}^{l_m,a_s}$ multiplied by the fields $\mathbf{v}^{l_m,a_s}$ of the two adjacent edges l_m sharing a_s.
- **Edge scalar functions**: the function $\varphi^{l_s,n}(\boldsymbol{\xi})$ appears in the composition of edge vector function $\boldsymbol{\Phi}^{l_s,n}$, multiplied by the field $\mathbf{v}^{l_m,\perp}$, and of the internal vectorial function $\boldsymbol{\Phi}^{K,l_s,n}$, multiplied by the field $\mathbf{v}^{l_s,\top}$.
- **Internal scalar functions**: the function $\varphi^{K,n_1,n_2}(\boldsymbol{\xi})$ appears in the composition of the internal vectorial functions $\boldsymbol{\Phi}^{K,n_1,n_2}_{(1)}$, $\boldsymbol{\Phi}^{K,n_1,n_2}_{(2)}$ multiplied by the fields $\mathbf{v}^K_{(j)}$ $j = 1, 2$, respectively.

It is worth noting the following properties of the vectorial shape functions in $\mathbf{B}^K_k$

- The edge shape functions $\boldsymbol{\Phi}^{l_m,a_s} = \varphi^{a_s}\mathbf{v}^{l_m,a_s}$ vanish at an edge l_q if a_s is not a vertex of l_q, since the scalar vertex function φ^{a_s} verifies this property. If a_s is a vertex of l_q and $l_m \neq l_q$ (l_q is adjacent to l_m), then the normal component $\langle \boldsymbol{\Phi}^{l_m,a_s}, \mathbf{n}\rangle|_{l_q} = 0$, given that the normal component of $\mathbf{v}^{l_m,a_s}$ is zero along the adjacent side of l_m by the vertex a_s. Over l_m, the normal component $\langle \boldsymbol{\Phi}^{l_m,a_s}, \mathbf{n}^K\rangle|_{l_m} = \varphi^{a_s}|_{l_m}$, keeping in mind that the normal component of $\mathbf{v}^{l_m,a_s}$ is unitary over l_m.
- The edge shape functions $\boldsymbol{\Phi}^{l_m,n} = \varphi^{l_m,n}\mathbf{v}^{l_m,\perp}$ vanish at l_q if $l_q \neq l_m$, considering that the edge of scalar function $\varphi^{l_m,n}$ has this property. About l_m, the normal component $\langle \Phi^{l_m,n}, \mathbf{n}^K\rangle|_{l_m} = \varphi^{l_m,n}|_{l_m}$, keeping in mind that the normal component of $\mathbf{v}^{l_m,\perp}$ is unitary along l_m.
- The internal shape functions $\boldsymbol{\Phi}^{K,l_m,n} = \varphi^{l_m,n}\mathbf{v}^{l_m,\top}$ vanish on all edges l_q, with $l_q \neq l_m$, since the edge scalar function $\varphi^{l_m,n}$ has this property. On l_m, the normal component $\langle \boldsymbol{\Phi}^{K,l,n}, \mathbf{n}^K\rangle|_{l_m}$ is zero, given that the normal component of $\mathbf{v}^{l_m,\top}$ is zero along l_m.
- The internal functions $\boldsymbol{\Phi}^{K,n_1,n_2}_{(j)} = \varphi^{K,n_1,n_2}\mathbf{v}^K_{(j)}$ vanish on all edges of K, since the internal scalar functions φ^{K,n_1,n_2} verify this property.

Theorem 5.4. *The set of vectorial functions $\mathbf{B}^K_k$ is linearly independent.*

Proof. Consider the linear combination

$$\begin{aligned}\mathbf{g} = &\sum_{l_m\in\mathcal{A}}\left[\sum_{a_s\in l_m}\alpha_{m,s}\boldsymbol{\Phi}^{l_m,a_s} + \sum_n \beta_{m,n}\boldsymbol{\Phi}^{l_m,n} + \sum_n \gamma_{m,n}\boldsymbol{\Phi}^{K,l_m,n}\right]\\ &+ \sum_{n_1,n_2}\lambda^{(1)}_{n_1,n_2}\boldsymbol{\Phi}^{K,n_1,n_2}_{(1)} + \sum_{n_1,n_2}\lambda^{(2)}_{n_1,n_2}\boldsymbol{\Phi}^{K,n_1,n_2}_{(2)} = 0.\end{aligned}$$

The expression of $\mathbf{g}$ can be grouped by the contributions of each of the scalar shape functions

$$\begin{aligned}\mathbf{g} = &\sum_{a_s\in\mathcal{V}}\left[\sum_{m;\ a_s\in\mathcal{V}_m}\alpha_{m,s}\mathbf{v}^{l_m,a_s}\right]\varphi^{a_s} + \sum_n\left[\sum_{l_m\in\mathcal{A}}\beta_{m,n}\mathbf{v}^{l_m,\perp} + \gamma_{m,n}\mathbf{v}^{l_m,\top}\right]\varphi^{l_m,n}\\ &+ \sum_{n_1,n_2}[\lambda^{(1)}_{n_1,n_2}\mathbf{v}^K_{(1)} + \lambda^{(2)}_{n_1,n_2}\mathbf{v}^K_{(2)}]\varphi^{K,n_1,n_2} = 0.\end{aligned}$$

Since the scalar shape functions are linearly independent, it follows that the vectorial coefficients multiplying each of these functions in the linear combination $\mathbf{g}$ vanish. That is,

$$\sum_{m;\ a_s\in\mathcal{V}_m}\alpha_{m,s}\mathbf{v}^{l_m,a_s} = 0, \tag{5.10}$$

$$\beta_{m,n}\mathbf{v}^{l_m,\perp} + \gamma_{m,n}\mathbf{v}^{l_m,\top} = 0, \tag{5.11}$$

$$\lambda^{(1)}_{n_1,n_2}\mathbf{v}^K_{(1)} + \lambda^{(2)}_{n_1,n_2}\mathbf{v}^K_{(2)} = 0. \tag{5.12}$$

Considering the property of linear independence of two fields associated with each vertex of (5.10), we have that $\alpha_{m,s} = 0$. Similarly, the linear independence property of the two fields associated with each edge, it follows from (5.11) that $\beta_{m,n} = \gamma_{m,n} = 0$. Finally, in view of the property of the linear independence of two fields associated with the volume, thus $\lambda^{(1)}_{n_1,n_2} = \lambda^{(2)}_{n_1,n_2} = 0$. Consequently, the set $\mathbf{B}^K_k$ turns out to be linearly independent. □

5.5. $\mathbf{H}(\mathrm{div})$-conforming subspaces

Let $\mathbf{u}^K \in \operatorname{span}\mathbf{B}^K_k \subset \mathbf{H}(\mathrm{div}, K)$ and consider the expansion

$$\mathbf{u}^K = \sum_{l_m\in\mathcal{A}}\left[\sum_{a_s\in l_m}\alpha_{m,s}\boldsymbol{\Phi}^{l_m,a_s} + \sum_n \beta_{m,n}\boldsymbol{\Phi}^{l_m,n} + \sum_n \gamma_{m,n}\boldsymbol{\Phi}^{K,l_m,n}\right] + \sum_{n_1,n_2}\lambda^{(1)}_{n_1,n_2}\boldsymbol{\Phi}^{K,n_1,n_2}_{(1)} + \sum_{n_1,n_2}\lambda^{(2)}_{n_1,n_2}\boldsymbol{\Phi}^{K,n_1,n_2}_{(2)}.$$

Let $K^\ell, K^j \in \Gamma$ be two neighboring elements sharing a common edge $l^{\ell,j} = K^\ell \cap K^j$. Recalling the properties of the normal components of each of the vectorial shape functions, the only terms contributing to this calculation of $\langle \mathbf{u}^K, \mathbf{n}^K\rangle|_{l^{\ell,j}}$ are drawn from the edge bases. Precisely, it follows that

$$\langle \mathbf{u}^K, \mathbf{n}^K\rangle|_{l^{\ell,j}} = \sum_{a_s\in\mathcal{V}^{l^{\ell,j}}}\alpha_{q,s}\varphi^{a_s}|_{l^{\ell,j}} + \sum_n \beta_{q,n}\varphi^{l^{\ell,j},n}|_{l^{\ell,j}}. \tag{5.13}$$

Thus, in view of the continuity of scalar bases at the interface $l^{\ell,j}$, the necessary and sufficient condition for the jump of the normal component to be zero is that the coefficients of the edge functions $\boldsymbol{\Phi}^{l^{\ell,j},a_s}$ associated with the vertex of $l^{\ell,j}$ and edge functions $\boldsymbol{\Phi}^{l^{\ell,j},n}$ associated with same edge $l^{\ell,j}$ are opposite in both elements K^ℓ and K^j sharing this interface. This result is summarized in following theorem.

Theorem 5.5. *Let Γ be a partition of the domain Ω formed by elements K, which are mapped from triangular or quadrilateral master elements, and consider hierarchical vectorial bases $\mathbf{B}^K_k$, defined in (5.9). Consider a space $\mathbf{V}^\Gamma_k$ of vectorial functions $\mathbf{u}$ such that $\mathbf{u}^K = \mathbf{u}|_K \in$ span $\mathbf{B}^K_k \subset \mathbf{H}(\mathrm{div}, K)$. Suppose that in the expansions of $\mathbf{u}^{K^\ell}$ and $\mathbf{u}^{K^j}$ with respect to the bases $\mathbf{B}^{K^\ell}_k$ and $\mathbf{B}^{K^\ell}_k$ of two neighboring elements $K^\ell, K^j \in \Gamma$, sharing a common edge $l^{\ell,j} = K^\ell \cap K^j$, the corresponding coefficients multiplying edge shape functions associated to $l^{\ell,j}$ in both elements K^ℓ and K^j are opposite. Then V^Γ_k is a subspace of $\mathbf{H}(\mathrm{div}, \Omega)$.*

6. Numerical applications

Consider the model Poisson problem expressed as:

$$\nabla\cdot\boldsymbol{\sigma} = f \quad \text{in } \Omega, \tag{6.1}$$

$$\boldsymbol{\sigma} = -\nabla u, \tag{6.2}$$

$$u = u_D \quad \text{in } \partial\Omega, \tag{6.3}$$

where $\Omega \subset \mathbb{R}^d$ is the computational domain.

Mixed formulation

As studied in [1], the mixed formulation for problem (6.1)–(6.3) is: find $(\boldsymbol{\sigma}, u) \in \left(\mathbf{H}(\mathrm{div}, \Omega) \times L^2(\Omega)\right)$ such that, for all $\mathbf{q} \in \mathbf{H}(\mathrm{div}, \Omega)$ and $\varphi \in L^2(\Omega)$,

$$\int_\Omega \boldsymbol{\sigma}.\mathbf{q}\, d\Omega - \int_\Omega u\nabla\cdot\mathbf{q}\, d\Omega = -\int_{\partial\Omega} u_D\mathbf{q}.\mathbf{n}ds, \tag{6.4}$$

$$\int_\Omega \nabla\cdot\boldsymbol{\sigma}\varphi\, d\Omega = \int_\Omega f\,\varphi\, d\Omega. \tag{6.5}$$

In typical $\mathbf{H}(\mathrm{div})$-conforming discretized versions of the mixed formulation, approximate solutions for dual $\boldsymbol{\sigma}$ and primal u variables are searched in finite dimensional subspaces $\mathbf{V}_h \subset \mathbf{H}(\mathrm{div}, \Omega)$ and $U_h \subset L^2(\Omega)$, which are based on a partition Γ_h of the computational domain Ω.

In order to simplify the computation of the integral terms involving the divergence operator, the implementation of the present paper proceeds as in discontinuous Galerkin formulations by splitting the integrals over the elements of the partition. By using integration by parts on the integral terms involving the divergence operator restricted to K, we get the

Table 2
Dimensions of vectorial approximation spaces of type $\vec{\mathcal{P}}_k$ and $\vec{\mathcal{P}}_k^{\,*}$ based on triangular and quadrilateral elements, and the number of edge and internal shape functions in each case.

Element	Type	Edge	Internal	Total
Triangular	$\vec{\mathcal{P}}_k$	$3(k+1)$	k^2-1	$(k+1)(k+2)$
	$\vec{\mathcal{P}}_k^{\,*}$	$3(k+1)$	$(k+1)^2-1$	$3+k(k+5)$
Quadrilateral	$\vec{\mathcal{P}}_k$	$4(k+1)$	$2(k^2-1)$	$2(k+1)^2$
	$\vec{\mathcal{P}}_k^{\,*}$	$4(k+1)$	$2k(k+1)$	$2(k+1)(k+2)$

expression

$$\int_K u\nabla\cdot\mathbf{q}\ dK = -\int_K \nabla u.\mathbf{q}\ dK + \int_{\partial K} u\mathbf{q}.\mathbf{n}^K\ ds,$$
$$\int_K \nabla\cdot\boldsymbol{\sigma}\varphi\ dK = -\int_K \nabla\varphi.\boldsymbol{\sigma}\ dK + \int_{\partial K} \varphi\boldsymbol{\sigma}.\mathbf{n}^K\ ds.$$

After that, these terms are inserted into Eqs. (6.1)–(6.3), and added over all elements of the partition, to obtain the following new formulation, without requiring divergence computations,

$$\sum_{K\in\Gamma}\left(\int_K(\boldsymbol{\sigma}.\mathbf{q}+\nabla u.\mathbf{q})\ dK\right) + \int_{\Lambda_{int}}[\![u]\!]\ \mathbf{q}.\eta\ ds + \int_{\partial\Omega}(u_D-u)\mathbf{q}.\mathbf{n}\ ds = 0,$$
$$\sum_{K\in\Gamma}\left(\int_K \nabla\varphi.\boldsymbol{\sigma}\ dK + \int_K f\varphi\ dx\right) - \int_{\Lambda_{int}}[\![\varphi]\!]\ \boldsymbol{\sigma}.\eta\ ds - \int_{\partial\Omega}\varphi\boldsymbol{\sigma}.\mathbf{n}\ ds = 0,$$

where Λ_{int} represents the set formed by the edges of the elements in Γ placed in the interior of Ω, and $[\![u]\!]|_{l^{\ell,j}} = u^{K^j}|_{l^{\ell,j}} - u^{K^\ell}|_{l^{\ell,j}}$ denotes the trace jump of u at an interface $l^{\ell,j}$ of two elements K^j and K^ℓ, η being an established direction, as stated in the definition of Eq. (4.4).

Approximation spaces

The purpose is to use finite element approximation spaces U_h and $\mathbf{V}_h$, based on curved triangular or quadrilateral meshes Γ_h with characteristic side length h, to solve the mixed formulation. The primal variable is approximated by functions in $U_h = U_k^{\Gamma_h} \subset L^2(\Omega)$, which are piecewise defined as $u|_K = \mathbb{F}_K\hat{u},\ \hat{u}\in\mathcal{P}_k$, for $K\in\Gamma_h$, without any continuity constraint. The dual variable $\boldsymbol{\sigma}$ is searched in subspaces $\mathbf{V}_h \subsetneq \mathbf{V}_{k+1}^{\Gamma_h}$.

In this way, the discrete version of the mixed formulation is conservative. However, it is well known that the set of approximations $(\mathbf{V}_h, U_h)$ should be consistent in order to produce stable approximations (e.g., inf–sup condition). In this sense, as in the De Rham complex, the effect of the exact sequence property

$$\nabla\cdot\mathbf{V}_h = U_h \tag{6.6}$$

on the stability of the mixed problem is crucial, as described in [7,9].

Denote by $\vec{\mathcal{P}}_k = [\mathcal{P}_k]^2$ the space of vectorial functions with components in $\mathcal{P}_k$. It is known that when the polynomials in $\mathcal{P}_k$ are of total degree k, then $\nabla\cdot\vec{\mathcal{P}}_{k+1} = \mathcal{P}_k$. For this reason, approximation spaces $(\mathbf{V}_h, U_h)$ based on polynomial spaces of type $\vec{\mathcal{P}}_{k+1}, \mathcal{P}_k$ are usually stable for triangular meshes, giving optimal convergence rates, in the L^2-norm, of orders $k+2$ and $k+1$ for dual and primal variables, respectively.

However, when $\mathcal{P}_k$ is of tensor-product polynomials of maximum degree k, then $\nabla\cdot\vec{\mathcal{P}}_{k+1} \supsetneq \mathcal{P}_k$. Consequently, approximation spaces $(\mathbf{V}_h, U_h)$ based on polynomial spaces of type $\vec{\mathcal{P}}_{k+1}, \mathcal{P}_k$ are not consistent when applied to quadrilateral meshes. For these geometries, consistent approximation spaces of type $\vec{\mathcal{P}}_k^*, \mathcal{P}_k$ are possible, giving optimal convergence rates of order $k+1$ for both dual and primal variables. These are the type of space configurations that were first introduced by Raviart–Thomas for quadrilateral geometries. The principle for the construction of polynomial spaces of type $\vec{\mathcal{P}}_k^*$ is to add to $\vec{\mathcal{P}}_k$ those vectorial polynomials of $\vec{\mathcal{P}}_{k+1}$, of maximum degree $k+1$, but with divergence in $\mathcal{P}_k$.

Table 2 indicates the dimensions of the vectorial polynomial spaces $\vec{\mathcal{P}}_k$ and $\vec{\mathcal{P}}_k^*$ for triangular and quadrilateral geometries, specifying the number of edge and internal shape functions in each case.

Extensions of these approximation settings for three-dimensional affine elements of tetrahedral, hexahedral and prismatic geometries are presented in [18], where another type of space configuration denoted by $\vec{\mathcal{P}}_k^{**}, \mathcal{P}_{k+1}$ is also considered, by further incrementing the degree of some internal flux functions to $k+2$, and matching primal functions to $k+1$ (higher than the border fluxes of degree k). In this new setting, higher convergence rate of order $k+2$ is obtained for the primal variable. Using static condensation, the global condensed matrices to be solved in both space configurations $\vec{\mathcal{P}}_k^*, \mathcal{P}_k$ and $\vec{\mathcal{P}}_k^{**}, \mathcal{P}_{k+1}$ have same dimension, proportional to the dimension of border fluxes.

Inspired by the principle adopted for affine meshes, the simulations presented in this paper are based on approximation spaces of type $\vec{\mathcal{P}}_k^*$, $\mathcal{P}_k$ for curvilinear meshes, both for triangular and quadrilateral geometries. This means that the dual variable $\boldsymbol{\sigma}$ is searched in approximation spaces $\mathbf{V}_h \subsetneq \mathbf{V}_{k+1}^{\Gamma_h}$ which are locally spanned by the edge vectorial shape functions in $\mathbf{B}_k^K$, and by those internal shape functions $\boldsymbol{\Phi} = \varphi\mathbf{v} \in \mathbf{B}_{k+1}^K$ corresponding to internal shape functions in the master element $\hat{\boldsymbol{\Phi}} = \hat{\varphi}\hat{\mathbf{b}} \in \vec{\mathcal{P}}_{k+1}$ having divergence in $\mathcal{P}_k$. With this procedure, that guarantees the validity of the relation (6.6) in the case of affine elements, we expect to produce stable simulations with optimal convergence rates for the case of curvilinear elements as well.

Static condensation

In all the cases, static condensation is applied to represent the discretized version of the mixed formulation. At each element K of the partition, consider the organization of the degrees of freedom of the flux in terms of $\boldsymbol{\sigma}_e$, and $\boldsymbol{\sigma}_i$ formed by internal and boundary fluxes. The pressure is represented by a scalar value u_0 and the degrees of freedom u_i of the pressure approximation except u_0. Thus, the local matrix representation can be expressed in the form

$$\left(\begin{array}{cc|cc} A_{ii} & B_{ii}^T & B_{ie}^T & A_{ie} \\ B_{ii} & 0 & 0 & B_{ie} \\ \hline B_{ie} & 0 & 0 & B_{ee} \\ A_{ei} & B_{ie}^T & B_{ee}^T & A_{ee} \end{array}\right) \left(\begin{array}{c} \boldsymbol{\sigma}_i \\ u_i \\ \hline u_0 \\ \boldsymbol{\sigma}_e \end{array}\right) = \left(\begin{array}{c} -f_{u_D} \\ -f_i \\ \hline -f_0 \\ 0 \end{array}\right),$$

where, f_{u_D} is the contribution to the right hand side of non-homogeneous Dirichlet boundary condition, f_i is the right hand side volume contribution associated to condensed scalar shape functions, f_0 being associated to the remaining ones. Then, static condensation may be applied by eliminating the internal degrees of freedom $\boldsymbol{\sigma}_i$ and u_i, to get a condensed system involving only equations for $\boldsymbol{\sigma}_e$ and u_0.

Problem 1. Curved elements on a circular region.

Consider the model problem defined on the circular region $\Omega \subset \mathbb{R}^2$ with radius $r = 1$. The exact solution is the harmonic function

$$u(r,\theta) = r^4\cos(2\theta)\sin(2\theta),$$
$$\boldsymbol{\sigma}(r,\theta) = -\begin{bmatrix} 4r^3\cos(2\theta)\sin(2\theta) \\ 2r^3\left(\cos^2(2\theta) - \sin^2(2\theta)\right) \end{bmatrix},$$

corresponding to the forcing term $f = 0$.

Starting with a partition of Ω formed by four curved triangular elements, covering the central disc with radius $r = 1/2$, and four curved rectangular elements, covering the annular region corresponding to $1/2 < r \leq 1$, the meshes are obtained by subsequent uniform subdivision of each element into four new subelements. Fig. 6.1(left side) illustrates the resulting curved meshes restricted to one quadrant of Ω.

Problem 2. Curved elements on a cylinder.

Consider a half cylindrical manifold $\Omega \subset \mathbb{R}^3$ with radius 1, corresponding to angle $0 \leq \theta \leq \pi$, and $-\frac{\pi}{2} \leq z \leq \frac{\pi}{2}$. The exact solution is defined by

$$u(\theta, z) = \sin(\theta)\cos(z),$$
$$\boldsymbol{\sigma}(\theta, z) = \begin{bmatrix} 0 \\ -\cos\theta\cos z \\ \sin\theta\sin z \end{bmatrix},$$

corresponding to the forcing term $f = 2\cos z\sin\theta$.

Starting with a partition of Ω into two cylindrical parts obtained by the subdivision of the angle variable at $\frac{\pi}{2}$, the meshes are subsequently defined by uniform subdivision, as illustrated in Fig. 6.1 (central side).

Problem 3. Curved elements on the unit sphere.

Consider the model problem on the unit sphere $\Omega \subset \mathbb{R}^3$, having exact solution given in spherical coordinates by

$$u(\theta, \phi) = \sin^6(\theta)(1 - \cos^2\phi),$$
$$\boldsymbol{\sigma}(\theta, \phi) = -\begin{bmatrix} 0 \\ \dfrac{6\cos\theta\sin^5\theta\sin^2\phi}{r} \\ \dfrac{\sin^5\theta\sin 2\phi}{r} \end{bmatrix},$$

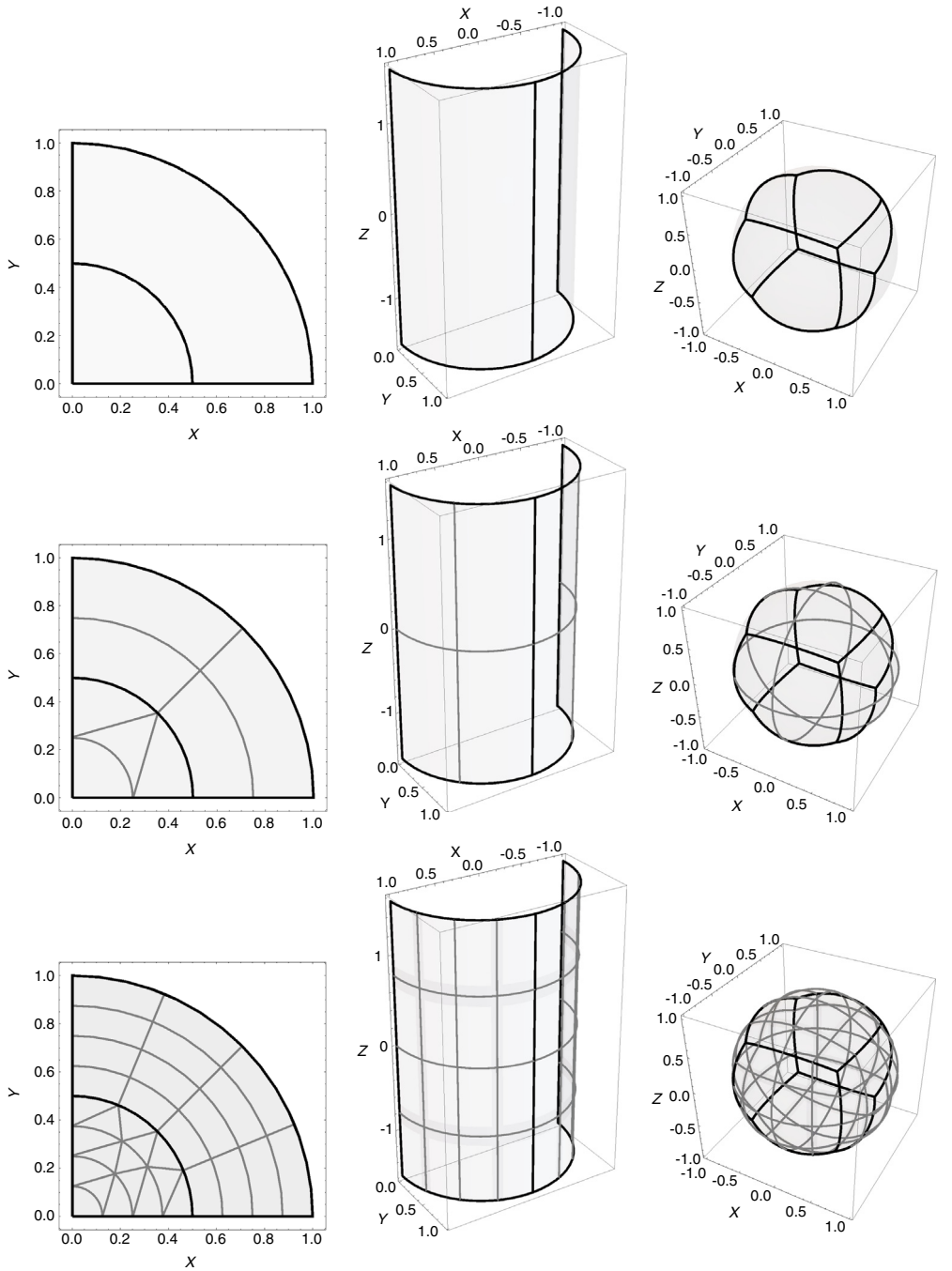

Fig. 6.1. Mesh geometries of one quadrant of the circular region Ω in Problem 1 (left), the cylindrical region in Problem 2 (center) and the unit sphere in Problem 3 (right), at refinement levels $L = 0, 1, 2$. Thick black curves refer to the coarser mesh, and gray lines correspond to refined mesh levels.

corresponding to the forcing term

$$f = -\frac{\sin^4\theta\left(-6\sin^2\theta + \cos^2\phi(2 + 6\sin^2\theta) + (-2 + 36\cos^2\theta)\sin^2\phi\right)}{r^2}.$$

The curved meshes are obtained by a projection of uniform meshes on the faces of a cube, as illustrated in Fig. 6.1 (right side). For this test case, $\partial\Omega$ corresponds to a line (slit) on the equator of the sphere. On this line a Dirichlet condition is applied corresponding to the exact solution.

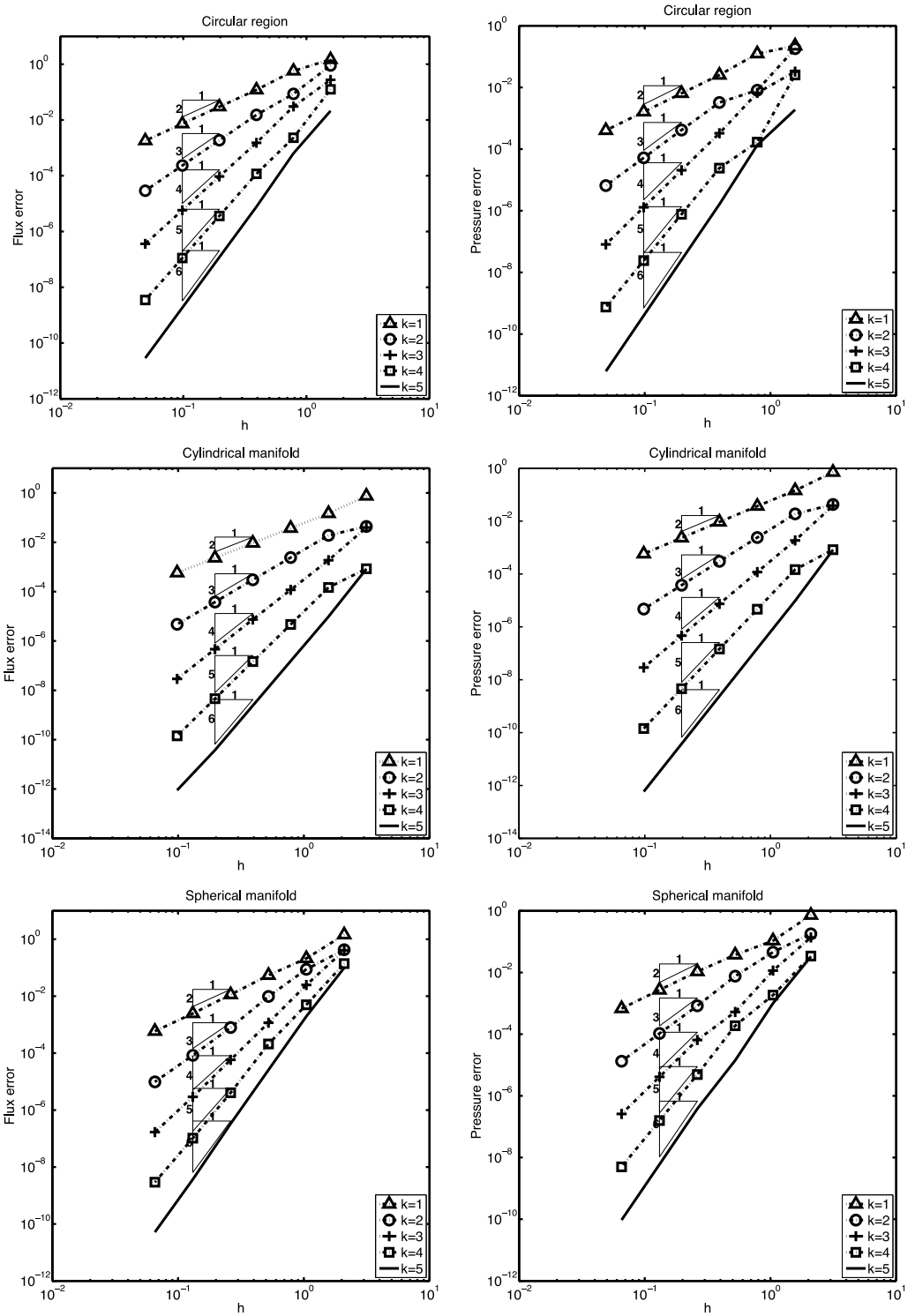

Fig. 6.2. Convergence histories for the flux (left side) and the pressure (right side) for Problem 1 (top), Problem 2 (center) and Problem 3 (bottom), using the mixed method with approximation space configurations of type $\vec{\mathcal{P}}_k^*,\ \mathcal{P}_k$, for $k = 1, 2, 3, 4$ and 5.

The results of the three problems are summarized in Fig. 6.2, demonstrating optimal convergence rates in the L^2-norm of order $k+1$, both for primal and dual variables. These results reveal that the set of approximation spaces $(\mathbf{V}_h, U_h)$ of type $\vec{\mathcal{P}}_k^*,\ \mathcal{P}_k$, used in the simulations, is stable.

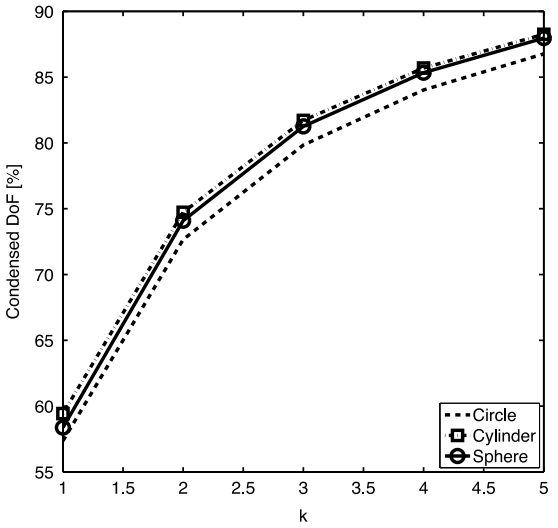

Fig. 6.3. Percentage of condensed degrees of freedom in the mixed method for Problem 1 (black line), Problem 2 (red line) and Problem 3 (blue line), at the finest refinement level.

Fig. 6.3 illustrates the effectiveness of the static condensation procedure in the reduction of degrees of freedom at the finest level of refinement. More degrees of freedom can be condensed when increasing the polynomial order. Quadrilateral elements have a larger number of *condensable* degrees of freedom. For instance, for $k = 5$, about 88% of the total number of degrees of freedom is condensed in the cylindrical and spherical manifolds, using quadrilateral elements, and about 87% for the circular region, using both quadrilateral and triangular elements.

7. Conclusions

A new approach is presented for developing **H**(div)-conforming approximation spaces for curved elements in two dimensional manifolds immersed in R^3. These approximations are *by nature* locally conservative.

The properties of the Piola transformation are used to define vector fields over the geometric elements which are tangent to the manifold, which are then combined with higher order H^1-conforming scalar shape functions to create high order **H**(div)-conforming approximation spaces on manifolds.

Static condensation has been applied to reduce the size of the global system of equations. It is shown that for approximations of order $k = 5$ more than 85% of the total number of equations can be locally condensed, making the mixed finite element approximations computationally more efficient.

In order to avoid loss of local conservation due to numerical integration errors, the mixed formulation is modified by applying an additional integration by parts locally on each element. This modified formulation avoids the need of computing the divergence of the flux shape functions.

The proposed approximation setting has been applied to a two dimensional problem over a circle and to two dimensional problems embedded in R^3 representing a cylindrical region and a sphere. For all simulated problems optimal convergence rates are observed.

Acknowledgments

The authors P.R.B. Devloo, A.M. Farias, S.M. Gomes and O. Durán thankfully acknowledge financial support from the Brazilian National Agency of Petroleum, Natural Gas and Biofuels (ANP—PETROBRAS, grant SAP4600333146). P.R.B. Devloo and S.M. Gomes thankfully acknowledge financial support from CNPq—the Brazilian Research Council (grants 310369/2006-1 and 308632/2006-0). D.A. Castro is grateful for the hospitality received during his pos-doc visit at LabMeC (Laboratório de Mecânica Computacional), FEC-Unicamp, when this paper was prepared, and for financial support received from FAPESP—the Research Foundation of the State of São Paulo, Brazil (grant 2013/21959-4).

References

[1] F. Brezzi, M. Fortin, Mixed and Finite Element Methods, in: Springer Series in Computational Mathematics, vol. 15, Springer-Verlag, New York, 1991.
[2] P.A. Raviart, J.M. Thomas, A mixed finite element method for 2-nd order elliptic problems, in: R. Glowinski, E.Y. Rodin, O.C. Zienkiewicz (Eds.), Em: Mathematical Methods in Finite Element Analysis, John Wiley and Sons, Chichester, 1979.
[3] M.E. Rognes, R.C. Kirby, A. Logg, Efficient assembly of **H**(div) and **H**(curl) conforming finite elements, SIAM J. Sci. Comput. 31 (6) (2009) 4130–4151.
[4] T. Abbogast, C.N. Dawson, P.T. Keenan, M.F. Weeler, I. Yotov, Enhanced cell-centered finite differences for elliptic equations on general geometry, SIAM J. Sci. Comput. 19 (2) (1998) 404–425.

[5] S. Pavel, K. Segeth, I. Dolezel, Higher-Order Finite Element Methods, Chapman-Hall/CRC, 2004.
[6] L. Demkowicz, Polynomial exact sequence and projection-based interpolation with application Maxwell equations, in: D. Boffi, L. Gastaldi (Eds.), Mixed Finite Elements, Compatibility Conditions and Applications, 2006, pp. 101–156.
[7] J. Schöberl, S. Zaglmayr, High order Nedelec elements with local complete sequence properties, Int. J. Comput. Math. Electr. Electron. Eng. 24 (2) (2005) 374–384.
[8] S. Zaglamayr, Hight order finite element methods for electromagnetic field computation (Ph.D. thesis), Johannes Keppler Universität Linz, 2006.
[9] F. Fuentes, B. Keith, L. Demkowicz, S. Nagaraj, Orientation embedded high order shape functions for the exact sequence elements of all shapes, Comput. Math. Appl. 70 (2015) 353–458.
[10] M.E. Rognes, D.A. Ham, C.J. Cotter, A.T.T. McRae, Automating the solution of PDEs on the sphere and other manifolds in FEniCS 1.2, Geosci. Model. Dev. 6 (2013) 2099–2119.
[11] D. Siqueira, P.R.B. Devloo, S.M. Gomes, A new procedure for the construction of Hdiv and Hcurl finite element spaces, J. Comput. Appl. Math. 240 (2013) 204–214.
[12] http://github.com/labmec/neopz.
[13] P.R.B. Devloo, C.M.A. Bravo, E.C. Rylo, Systematic and generic construction of shape functions for *p*-adaptive meshes of multidimensional finite elements, Comput. Methods Appl. Mech. Engrg. 198 (2009) 1716–1725.
[14] J.L.D. Calle, P.R.B. Devloo, S.M. Gomes, Implementation of continuous hp-adaptive finite element spaces without limitations on hanging sides and distribution of approximation orders, Comput. Math. Appl. 70 (5) (2015) 1051–1069.
[15] A.M. Farias, Novas formulações de elementos finitos e simulações multifísicas (Doctorate Thesis), IMECC-Unicamp, 2014.
[16] P.C.A. Lucci, Descrição matemática de geometrias curvas por interpolação transfinita Dissertação de Mestrado, FEC-Unicamp, 2009.
[17] W.J. Gordon, C.A. Hall, Transfinite element methods: Blending function interpolation over arbitrary curved element domains, Numer. Math. 21 (2) (1973) 109–129.
[18] D.A. Castro, P.R.B. Devloo, A.M. Farias, S.M. Gomes, D. Siqueira, Three dimensional hierarchical mixed finite element approximations with enhanced primal variable accuracy. Report 2015. http://www.labmec.org.br/wiki/publicacoes/report/douglas-castro.